ARTICLE IN PRESS

Journal of Computational Physics xxx (2012) xxx–xxx

Contents lists available at SciVerse ScienceDirect

Journal of Computational Physics

journal homepage: www.elsevier.com/locate/jcp

Non-linear Petrov–Galerkin methods for reduced order hyperbolic equations and discontinuous finite element methods

F. Fang [a], C.C. Pain [a], I.M. Navon [b,*], A.H. Elsheikh [a], J. Du [a,c], D. Xiao [a]

[a] Applied Modelling and Computation Group, Department of Earth Science and Engineering, Imperial College London, Prince Consort Road, London SW7 2BP, UK
[b] Department of Scientific Computing, Florida State University, Tallahassee, FL 32306-4120, USA
[c] The Institute of Atmospheric Physics, The Chinese Academy of Sciences, Beijing, China

ARTICLE INFO

Article history:
Received 16 March 2012
Received in revised form 3 October 2012
Accepted 12 October 2012
Available online xxxx

Keywords:
Finite element
Petrov–Galerkin
Proper orthogonal decomposition
Reduced order modelling
Shock wave

ABSTRACT

A new Petrov–Galerkin approach for dealing with sharp or abrupt field changes in discontinuous Galerkin (DG) reduced order modelling (ROM) is outlined in this paper. This method presents a natural and easy way to introduce a diffusion term into ROM without tuning/optimising and provides appropriate modelling and stablisation for the numerical solution of high order nonlinear PDEs. The approach is based on the use of the cosine rule between the advection direction in Cartesian space–time and the direction of the gradient of the solution. The stabilization of the proper orthogonal decomposition (POD) model using the new Petrov–Galerkin approach is demonstrated in 1D and 2D advection and 1D shock wave cases. Error estimation is carried out for evaluating the accuracy of the Petrov–Galerkin POD model. Numerical results show the new nonlinear Petrov–Galerkin method is a promising approach for stablisation of reduced order modelling.

1. Introduction

Reduced order model (ROM) technology is a rapidly growing discipline, with significant potential advantages in: interactive use, emergency response, ensemble calculations and data assimilation [1–4]. ROM is expected to play a major role in facilitating real-time turn-around with computational results and data assimilation. Most model reduction methods can be viewed as approximation methods by projection (for comprehensive description see [5,6]). Most of those methods (e.g., balanced truncation) are designed for stable, linear and moderate-order systems (state orders are less than 10^4) [7], so are not practical for many fluids systems although they can provide accurate low-order representations of state-space systems. Among existing approaches, the proper orthogonal decomposition (POD) method provides an efficient means of deriving the reduced basis for nonlinear partial differential equations (PDEs). Using the POD technique, it is possible to extract a set of modes characteristic of the database which constitutes the optimal basis for the energetic description of the flow. A Galerkin projection of the original equations onto a finite number of POD bases yields a set of ordinary differential equations in time. However, due to the energetic optimality of the POD bases, only few modes are sufficient to give a good representation of the kinetic energy of the flow. The leading POD modes are not able to dissipate enough energy since the main amount of viscous dissipation takes place in the small eddies (unresolved modes) [9]. Galerkin POD methods may thus suffer from a lack of numerical stability especially for high order nonlinear PDEs. There are various ways to recover the effect of the truncated bases (usually the small scales, i.e. unresolved modes) and improve the numerical stability by:

* Corresponding author. Tel.: +1 850 644 6560; fax: 1 850 644 0098.
E-mail addresses: inavon@fsu.edu, navon@scs.fsu.edu (I.M. Navon).
URL: http://amcg.ese.imperial.ac.uk (I.M. Navon).

0021-9991/$ - see front matter © 2012 Elsevier Inc. All rights reserved.
http://dx.doi.org/10.1016/j.jcp.2012.10.011

1. incorporating gradients as well as function values in the definition of POD [10,11];
2. adding calibrated/diffusion terms (*e.g.* eddy-viscosities, subgrid-scale model, streamline diffusion) into the POD reduced order equations [12,13];
3. the approach of Noack et al. [14], that uses a finite-time thermodynamics formalism;
4. residual based stablisation approach [9] where the unsolved terms are represented by a number of residual modes which are calculated by the residuals of ROMs.

For efficient calculation of nonlinear terms, the discrete empirical interpolation method (DEIM) [15] provides a dimension reduction of the nonlinear term by replacing the non-linear terms with a coefficient-function approximation consisting of a linear combination of pre-computed basis functions and parameter-dependent coefficients.

However the main drawback of the above stabilization methods is that there are always some parameters to tune/optimise for a best match the full solution. More recently, the Petrov–Galerkin method has been introduced to POD and applied to the 1D non-linear static problem and ODE [16]. This method presents a natural and easy way to introduce a diffusion term into ROM without tuning/optimising and provides appropriate modelling and stabilizations for the numerical solution of high order nonlinear PDEs.

In this paper, a new Petrov–Galerkin POD method is presented for non-linearity discontinuous Galerkin modelling in order to control numerical oscillations. The approach is based on the use of the cosine rule between the advection direction in Cartesian space–time and the direction of the gradient of the solution.

The remainder of this paper is organised as follows. Section 2 provides the derivation of the new Petrov–Galerkin approach for one scalar time dependent transport equation. This is then followed by the extension to coupled time dependent equations and an example is provided by two-time level discrete equations in Section 3. Section 4 addresses the issue of how stable reduced order modelling is performing using the new Petrov–Galerkin approach. In Section 5, a Bassi Rebay representation of discontinuous Galerkin methods for the diffusion term is described. The method is applied to 1D and 2D advection and shock cases in Section 6 followed by discussion of the numerical results. Finally, conclusions are drawn in Section 7.

2. Scalar equation

2.1. Non-linear Petrov–Galerkin scalar equation

The one scalar time dependent transport equation assumes the form:

$$\mathbf{a}_{xt} \cdot \nabla_{xt}\psi = s, \tag{1}$$

where ψ represents field states (*e.g.* temperature, pollutants); s is the source term; $\mathbf{a}_{xt} = (a_t\ \mathbf{a})^T$ and $\mathbf{a} = (a_x\ a_y\ a_z)^T$ (here, the velocity vector); a_t, a_x, a_y, a_z are the coefficients of the time and space derivatives along the x, y, z direction respectively. For simplicity, this Eq. (1) in 1D with time dependence becomes:

$$a_t \frac{\partial \psi}{\partial t} + a_x \frac{\partial \psi}{\partial x} = s. \tag{2}$$

Using the cosine rule between the two vectors $\mathbf{a}_{xt}$ and $\nabla_{xt}\psi$:

$$cos(\theta_a) = \frac{\mathbf{a}_{xt} \cdot \nabla_{xt}\psi}{|\mathbf{a}_{xt}|\,|\nabla_{xt}\psi|}, \tag{3}$$

where θ_a is the angle between the two vectors $\mathbf{a}_{xt}$ and $\nabla_{xt}\psi$. The projection of $\mathbf{a}_{xt}$ onto $\nabla_{xt}\psi$ can be written: $\mathbf{a}^*_{xt} = |\mathbf{a}_{xt}|\mathbf{n}_a cos(\theta_a)$ (here $\mathbf{n}_a = \frac{\nabla_{xt}\psi}{|\nabla_{xt}\psi|}$). Taking into account (3), it is then written:

$$\mathbf{a}^*_{xt} = \frac{(\mathbf{a}_{xt} \cdot \nabla_{xt}\psi)\nabla_{xt}\psi}{\|\nabla_{xt}\psi\|_2^2}, \tag{4}$$

where $\|\cdot\|$ represents the L_2 norm of a vector-valued function. Thus

$$\mathbf{a}^*_{xt} \cdot \nabla_{xt}\psi = \mathbf{a}_{xt} \cdot \nabla_{xt}\psi. \tag{5}$$

Using the Petrov–Galerkin approach, a modified form of the differential Eq. (2) can be written:

$$(1 - \nabla_{xt} \cdot \mathbf{a}^*_{xt} p^*_{xt})(\mathbf{a}_{xt} \cdot \nabla_{xt}\psi - s) = 0, \tag{6}$$

where the scalar p^*_{xt} is a function of $\mathbf{a}^*_{xt}$ and the size and shape of the elements see Eqs. (9), (13) and (14) below. Multiplying Eq. (6) by a space–time basis function N_{xti} at node i and integrating it by parts over a single element V_E with boundary Γ_E (here discontinuous Galerkin (DG) methods are employed), the discrete form of the scalar equation is written:

$$\int_{V_E} N_{xti} r dV - \int_{\Gamma_E} N_{xti}(\mathbf{n}_{xt} \cdot \mathbf{a}_{xt})^-(\psi - \psi_{bc}) d\Gamma + \int_{V_E} (\nabla_{xt} N_{xti}) \cdot \mathbf{a}^*_{xt} p^*_{xt} r dV - \int_{\Gamma_E} N_{xti} \mathbf{n}_{xt} \cdot \mathbf{a}^*_{xt} p^*_{xt} r d\Gamma = 0 \tag{7}$$

Please cite this article in press as: F. Fang et al., Non-linear Petrov–Galerkin methods for reduced order hyperbolic equations and discontinuous finite element methods, J. Comput. Phys. (2012), http://dx.doi.org/10.1016/j.jcp.2012.10.011

with a finite element expansion $\psi = \sum_{j=1}^{\mathcal{N}} N_{xtj}\psi_j$ and $r = \mathbf{a}_{xt}\cdot\nabla_{xt}\psi - s$ and $\mathbf{n}_{xt}$ is the normal to the element in space–time and $(\mathbf{n}_{xt}\cdot\mathbf{a}_{xt})^- = min\{0, \mathbf{n}_{xt}\cdot\mathbf{a}_{xt}\}$ enables the incoming boundary information to be defined. Applying a zero boundary condition for the residual $r = 0$ on Γ_E, results in:

$$\int_{V_E} N_{xti} r dV - \int_{\Gamma_E} (\mathbf{n}_{xt}\cdot\mathbf{a}_{xt})^- N_{xti}(\psi - \psi_{bc}) d\Gamma + \int_{V_E} (\nabla_{xt} N_{xti})\cdot\mathbf{a}^*_{xt} p^*_{xt} r dV = 0. \tag{8}$$

Using the finite element space–time Jacobian matrix $\mathbf{J}_{xt}$, the scalar p^*_{xt} in (6) can be calculated as [20]:

$$p^*_{xt} = \frac{1}{4}(\|\mathbf{J}^{-1}_{xt}\mathbf{a}^*_{xt}\|_2)^{-1}. \tag{9}$$

The finite element space–time Jacobian matrix for 3D time dependent problems is:

$$\mathbf{J}_{xt} = \begin{pmatrix} \frac{\partial t}{\partial t'} & \frac{\partial x}{\partial t'} & \frac{\partial y}{\partial t'} & \frac{\partial z}{\partial t'} \\ \frac{\partial t}{\partial x'} & \frac{\partial x}{\partial x'} & \frac{\partial y}{\partial x'} & \frac{\partial z}{\partial x'} \\ \frac{\partial t}{\partial y'} & \frac{\partial x}{\partial y'} & \frac{\partial y}{\partial y'} & \frac{\partial z}{\partial y'} \\ \frac{\partial t}{\partial z'} & \frac{\partial x}{\partial z'} & \frac{\partial y}{\partial z'} & \frac{\partial z}{\partial z'} \end{pmatrix}, \tag{10}$$

where the variables with $\prime$ are the local variables. For uniform space–time resolution with a time step size of Δt and an element size of Δx (in the x-direction), Δy (in the y-direction), Δz (in the z-direction), then:

$$\mathbf{J}_{xt} = \begin{pmatrix} \frac{1}{2}\Delta t & 0 & 0 & 0 \\ 0 & \frac{1}{2}\Delta x & 0 & 0 \\ 0 & 0 & \frac{1}{2}\Delta y & 0 \\ 0 & 0 & 0 & \frac{1}{2}\Delta z \end{pmatrix}. \tag{11}$$

The value of p^*_{xt} can be adjusted to ensure that the resulting value of p^*_{xt} is not so large that there is more transport backwards than forwards in the resulting discrete system of equations using:

$$p^*_{xt} = min\left\{\frac{1}{\epsilon}, \frac{1}{4}(\|\mathbf{J}^{-1}_{xt}\mathbf{a}^*_{xt}\|_2)^{-1}\right\}. \tag{12}$$

in which $\epsilon > 0$ and ϵ is a tolerance used to avoid a "division by zero" error, here $\epsilon = 1\times10^{-10}$. Due to increasing number of nodes, associated with DG, similar to the quadratic FE, continuous Petrov–Galerkin formulations use a factor of $\frac{1}{2}$ instead of $\frac{1}{4}$ in Eq. (12). The value of $\frac{1}{4}$ eliminates the downwind coupling (in 1-D) for pure advection at the inflow node of an element. This correctly centres the equation residual at the centre of mass of the basis function, for continuous finite element representations. In the present work, where discontinuous finite elements are used to formulate the space–time discretisation, the centre of mass of the basis function is centred at a distance of $\frac{\Delta x}{4}$ from the upwind boundary of the element. In the traditional Petrov Galerkin method $\mathbf{a}^*_{xt} = \mathbf{a}_{xt}$ in the above and $p_{xt} = \frac{1}{4}(|\mathbf{A}_{xt}\cdot\nabla_{xt}\mathbf{N}_{xti}|)^{-1}$ replaces p^*_{xt}.

An approximate expression to p^*_{xt} is obtained from the Riemann finite element method (for details, see [19]):

$$p^*_{xt} = \frac{1}{4}(|\mathbf{a}^*_{xt}\cdot\nabla_{xt}N_{xti}|)^{-1}. \tag{13}$$

This will pick up the shape function which is aligned with the direction of $\mathbf{a}^*_{xt}$ at least for elements with equal sized edges. Alternatively one can produce an p^*_{xt} that is independent of i with:

$$p^*_{xt} = min_k\left\{\frac{1}{4}(|\mathbf{a}^*_{xt}\cdot\nabla_{xt}N_{xtk}|)^{-1}\right\}. \tag{14}$$

Note that this expression uses the length scale of the element in the direction of $\mathbf{a}^*_{xt}$.

In the above we can work with the stabilization in the diffusion form with:

$$\int_{V_E} N_{xti} r dV - \int_{\Gamma_E} N_{xti}(\mathbf{n}_{xt}\cdot\mathbf{a}_{xt})^-(\psi - \psi_{bc}) d\Gamma + \int_{V_E} (\nabla_{xt}N_{xti})^T \nu \nabla_{xt}\psi dV = 0, \tag{15}$$

where ψ_{bc} represents the value of ψ at the boundary, and the scalar diffusion coefficient assumes the form:

$$\nu = \frac{(\mathbf{a}_{xt}\cdot\nabla_{xt}\psi)p^*_{xt} r}{\|\nabla_{xt}\psi\|^2}. \tag{16}$$

The diffusion coefficient ν can be modified to ensure positive diffusion with:

$$\nu = \frac{max\{0, (\mathbf{a}_{xt}\cdot\nabla_{xt}\psi)p^*_{xt} r\}}{\|\nabla_{xt}\psi\|^2}, \tag{17}$$

Please cite this article in press as: F. Fang et al., Non-linear Petrov–Galerkin methods for reduced order hyperbolic equations and discontinuous finite element methods, J. Comput. Phys. (2012), http://dx.doi.org/10.1016/j.jcp.2012.10.011

or working only with the residual by replacing $\mathbf{a}_{xt} \cdot \nabla_{xt}\psi$ with the residual r which results in:

$$v = \frac{r p^*_{xt} r}{\|\nabla_{xt}\psi\|^2}. \tag{18}$$

The diffusion coefficient v is always non-negative because p^*_{xt} is non-negative. Eq. (18) for the diffusivity can be derived by re-defining $\mathbf{a}^*_{xt}$ in (4) to be:

$$\mathbf{a}^*_{xt} = \frac{r\nabla_{xt}\psi}{\|\nabla_{xt}\psi\|^2}. \tag{19}$$

Note that then $\mathbf{a}^*_{xt} \cdot \nabla_{xt}\psi = \frac{r\nabla_{xt}\psi}{\|\nabla_{xt}\psi\|^2} \cdot \nabla_{xt}\psi = r$.

2.2. Simplified scalar equations

Using the two level time-stepping θ-method the residual is:

$$r = a_t \frac{\psi^{n+1} - \psi^n}{\Delta t} + \mathbf{a} \cdot \nabla\psi^{n+\theta} - s^{n+\theta}, \tag{20}$$

where $\theta = 0.5$, $\psi^{n+\theta} = \theta\psi^{n+1} + (1-\theta)\psi^n$ ($\theta \in [0,1]$) and

$$\nabla_{xt}\psi = \left(\frac{\psi^{n+1} - \psi^n}{\Delta t},\ (\nabla\psi^{n+\theta})^T\right)^T, \tag{21}$$

which enables the formalism of space–time discretisation to be applied, for example:

$$\mathbf{a}^*_{xt} = (a^*_t,\ \mathbf{a}^{*T})^T = \frac{(\mathbf{a}_{xt} \cdot \nabla_{xt}\psi)\nabla_{xt}\psi}{\|\nabla_{xt}\psi\|_2^2}, \tag{22}$$

and

$$p^*_{xt} = min\left\{\frac{1}{\epsilon}, \frac{1}{4}(\|\mathbf{J}^{-1}\mathbf{a}^*\|_2)^{-1}\right\}, \tag{23}$$

in which $\mathbf{J}$ is the block part of the matrix $\mathbf{J}_{xt}$ that is associated with Cartesian space. The stabilized discrete equations in the diffusion form can be expressed in Cartesian space:

$$\int_{V_E} N_i r dV - \int_{\Gamma_E} N_i(\mathbf{n} \cdot \mathbf{a})^-(\psi^{n+\theta} - \psi^{n+\theta}_{bc})d\Gamma + \int_{V_E} (\nabla N_i)^T v \nabla\psi^{n+1} dV = 0, \tag{24}$$

or in a form where we apply integration by parts of the transport terms once:

$$\begin{aligned}&\int_{V_E} N_i(a_t(\frac{\psi^{n+1} - \psi^n}{\Delta t}) - s^{n+\theta})dV - \int_{V_E} \nabla \cdot (N_i\mathbf{a})\psi^{n+\theta} dV + \int_{\Gamma_E} N_i(\mathbf{n} \cdot \mathbf{a})^-(\psi^{n+\theta}_{bc})d\Gamma \\ &+ \int_{\Gamma_E} N_i(\mathbf{n} \cdot \mathbf{a})^+\psi^{n+\theta} d\Gamma + \int_{V_E} (\nabla N_i)^T v \nabla\psi^{n+1} dV = 0.\end{aligned} \tag{25}$$

3. Coupled equations

3.1. Non-linear Petrov–Galerkin coupled equations

The Petrov–Galerkin method discussed above is further applied to the time dependent coupled transport equations:

$$\mathbf{A}_{xt} \cdot \nabla_{xt}\Psi = \mathbf{s}, \tag{26}$$

where for 1D $\mathbf{A}_{xt} = (\mathbf{A}_t\ \mathbf{A}_x)^T$ and in 3D $\mathbf{A}_{xt} = (\mathbf{A}_t\ \mathbf{A}_x\ \mathbf{A}_y\ \mathbf{A}_z)^T$ in which the matrices $\mathbf{A}_t, \mathbf{A}_x$, $\mathbf{A}_y$ and $\mathbf{A}_z$ contain the coefficients of the derivatives of scalars with respect to time t, coordinates x, y and z respectively. In 1D Eq. (26) becomes:

$$\mathbf{A}_t \frac{\partial\Psi}{\partial t} + \mathbf{A}_x \frac{\partial\Psi}{\partial x} = \mathbf{s}. \tag{27}$$

For coupled equations the projection of $\mathbf{A}_{xt}$ onto $\nabla_{xt}\Psi$ can be written:

$$\mathbf{A}^*_{xt} = \mathbf{V}(\mathbf{A}_{xt} \cdot \nabla_{xt}\Psi)\mathbf{V}(\|\nabla_{xt}\Psi\|_2^2)^{-1}\nabla_{xt}\Psi. \tag{28}$$

Thus

$$\mathbf{A}^*_{xt} \cdot \nabla_{xt}\Psi = \mathbf{A}_{xt} \cdot \nabla_{xt}\Psi, \tag{29}$$

Please cite this article in press as: F. Fang et al., Non-linear Petrov–Galerkin methods for reduced order hyperbolic equations and discontinuous finite element methods, J. Comput. Phys. (2012), http://dx.doi.org/10.1016/j.jcp.2012.10.011

or

$$\left(\mathbf{V}(\mathbf{A}_{xt}\cdot\nabla_{xt}\Psi)\mathbf{V}(\|\nabla_{xt}\Psi\|_2^2)^{-1}\nabla_{xt}\Psi\right)\cdot\nabla_{xt}\Psi=\mathbf{A}_{xt}\cdot\nabla_{xt}\Psi, \tag{30}$$

where $\mathbf{V}(\mathbf{g})$ is a diagonal matrix in which $\mathbf{V}(\mathbf{g})_{\mu\mu}=\mathbf{g}_\mu$ and the vector $\|\nabla_{xt}\Psi\|_2^2$ is such that the μth entry is $\|\nabla_{xt}\Psi\|_{2\mu}^2=(\nabla_{xt}\Psi_\mu)\cdot(\nabla_{xt}\Psi_\mu)$. Since the matrix $\mathbf{A}^*_{xt}$ has a block diagonal structure the transport Eqs. (26) are a set of $\mathcal{M}$ independent scalar equations in which the μth scalar equation is expressed as:

$$a^*_{t\,\mu}\frac{\partial\Psi_\mu}{\partial t}+a^*_{x\mu}\frac{\partial\Psi_\mu}{\partial x}+a^*_{y\,\mu}\frac{\partial\Psi_\mu}{\partial y}+a^*_{z\mu}\frac{\partial\Psi_\mu}{\partial z}=\mathbf{s}_\mu, \tag{31}$$

and $a^*_{t\,\mu}=\mathbf{A}^*_{t\mu\mu}$, $a^*_{x\mu}=\mathbf{A}^*_{x\mu\mu}$, $a^*_{y\,\mu}=\mathbf{A}^*_{y\mu\mu}$, $a^*_{z\mu}=\mathbf{A}^*_{z\mu\mu}$. Since the equations have been uncoupled then the scalar equation methods described in the previous section can now be applied. This is effectively done below.

The Petrov–Galerkin modified form of the differential equation is:

$$(\mathbf{I}-(\nabla_{xt}\cdot\mathbf{A}^*_{xt})^T\mathbf{P}^*_{xt})(\mathbf{A}_{xt}\cdot\nabla_{xt}\Psi-\mathbf{s})=\mathbf{0}, \tag{32}$$

where $\mathbf{I}$ is the $\mathcal{M}\times\mathcal{M}$ identity matrix. Testing Eq. (32) with a diagonal matrix of space–time basis function $\mathbf{N}_{xti}$ (this has the basis function $N_{xt\,i}$ along its main diagonal), integrating over a single element V_E and applying integration by parts results in:

$$\int_{V_E}\mathbf{N}_{xti}\mathbf{r}dV-\int_{\Gamma_E}\mathbf{N}_{xti}(\mathbf{n}_{xt}\cdot\mathbf{A}_{xt})^-(\Psi-\Psi_{bc})d\Gamma+\int_{V_E}((\nabla_{xt}\mathbf{N}_{xti})\cdot\mathbf{A}^*_{xt})^T\mathbf{P}^*_{xt}\mathbf{r}dV+\int_{\Gamma_E}\mathbf{N}_{xti}\mathbf{n}_{xt}\cdot\mathbf{A}^*_{xt}\mathbf{P}^*_{xt}\mathbf{r}d\Gamma=\mathbf{0}, \tag{33}$$

with a finite element expansion $\Psi=\sum_{j=1}^{\mathcal{N}}\mathbf{N}_{xtj}\Psi_j$ (where Ψ_j is the order $\mathcal{M}$ vector of unknowns at node j) and $\mathbf{r}=\mathbf{A}_{xt}\cdot\nabla_{xt}\Psi-\mathbf{s}$.

Using the eigen-decomposition $\mathbf{n}_{xt}\cdot\mathbf{A}_{xt}=\mathbf{L}_{xt}\Lambda_{xt}\mathbf{R}_{xt}$ then $(\mathbf{n}_{xt}\cdot\mathbf{A}_{xt})^-=\mathbf{L}_{xt}\Lambda^-_{xt}\mathbf{R}_{xt}$ with $\Lambda^-_{xtkk}=min\{0,\Lambda_{xtkk}\}$, where Λ_{xt} is the diagonal matrix whose diagonal elements are the corresponding eigenvalues, and

$$\mathbf{A}_{xt}\mathbf{R}_{xt}=\mathbf{L}_{xt}\Lambda_{xt};\quad\mathbf{A}^T_{xt}\mathbf{L}_{xt}=\mathbf{R}_{xt}\Lambda_{xt}, \tag{34}$$

where the matrices $\mathbf{L}_{xt}$ and $\mathbf{R}_{xt}$, whose columns are the normalised singular vectors, satisfy $\mathbf{L}^T_{xt}\mathbf{L}_{xt}=\mathbf{I}$ and $\mathbf{R}^T_{xt}\mathbf{R}_{xt}=\mathbf{I}$. This eigen decomposition enables the boundary condition to be applied to incoming information only. We apply a zero boundary condition for the residual $\mathbf{r}=\mathbf{0}$ which results in:

$$\int_{V_E}\mathbf{N}_{xti}\mathbf{r}dV-\int_{\Gamma_E}\mathbf{N}_{xti}(\mathbf{n}_{xt}\cdot\mathbf{A}_{xt})^-(\Psi-\Psi_{bc})d\Gamma+\int_{V_E}((\nabla_{xt}\mathbf{N}_{xti})\cdot\mathbf{A}^*_{xt})^T\mathbf{P}^*_{xt}\mathbf{r}dV=\mathbf{0}. \tag{35}$$

$\mathbf{P}^*_{xt}$ is a function of $\mathbf{A}^*_{xt}$ and the size and shape of the elements, for example:

$$\mathbf{P}^*_{xt}=\frac{1}{4}(|\mathbf{A}^*_{xt}\cdot\nabla_{xt}\mathbf{N}_{xti}|)^{-1}, \tag{36}$$

or using the space–time Jacobian matrix $\mathbf{J}_{xt}$:

$$\mathbf{P}^*_{xt}=\frac{1}{4}(\|\mathbf{J}^{-1}_{xt}\mathbf{A}^*_{xt}\|_2)^{-1}, \tag{37}$$

where $\mathbf{A}^*_{xt}=(\mathbf{A}^{*T}_t,\mathbf{A}^{*T}_x,\mathbf{A}^{*T}_y,\mathbf{A}^{*T}_z)^T$. Since the matrices $\mathbf{A}^*_t,\mathbf{A}^*_x,\mathbf{A}^*_y,\mathbf{A}^*_z$ are diagonal the matrix $\mathbf{P}^*_{xt}$ is also diagonal. In the traditional Petrov Galerkin method $\mathbf{A}^*_{xt}=\mathbf{A}_{xt}$ in the above and $\mathbf{P}_{xt}$ replaces $\mathbf{P}^*_{xt}$. In a similar way to the scalar equation, the value of $\mathbf{P}^*_{xt}$ can be adjusted to ensure that the resulting value of $\mathbf{P}^*_{xt}$ is not so large that there is more transport backwards than forwards in the resulting discrete system of equations by:

$$\mathbf{P}^*_{xt}=min\left\{\mathbf{E}^{-1},\frac{1}{4}(\|\mathbf{J}^{-1}_{xt}\mathbf{A}^*_{xt}\|_2)^{-1}\right\}, \tag{38}$$

where the diagonal entries of the matrix $\mathbf{E}$ are positive and $\mathbf{E}$ contains small positive numbers (tolerances) used to avoid a "division by zero or near zero" error, *e.g.* 1×10^{-10}.

In the above we can work with the stabilization in the diffusion form with:

$$\int_{V_E}\mathbf{N}_{xti}\mathbf{r}dV-\int_{\Gamma_E}\mathbf{N}_{xti}(\mathbf{n}_{xt}\cdot\mathbf{A}_{xt})^-(\Psi-\Psi_{bc})d\Gamma+\int_{V_E}(\nabla_{xt}\mathbf{N}_{xti})^T\mathbf{K}\nabla_{xt}\Psi dV=\mathbf{0}, \tag{39}$$

or in a form where we apply integration by parts of the transport terms once:

$$\int_{V_E}\mathbf{N}_{xti}(-\mathbf{s})dV-\int_{V_E}(\nabla_{xt}\cdot(\mathbf{N}_{xti}\mathbf{A}_{xt}))\Psi dV+\int_{\Gamma_E}\mathbf{N}_{xti}(\mathbf{n}_{xt}\cdot\mathbf{A}_{xt})^-\Psi_{bc}d\Gamma+\int_{\Gamma_E}\mathbf{N}_{xti}(\mathbf{n}_{xt}\cdot\mathbf{A}_{xt})^+\Psi d\Gamma$$
$$+\int_{V_E}(\nabla_{xt}\mathbf{N}_{xti})^T\mathbf{K}\nabla_{xt}\Psi dV=\mathbf{0}, \tag{40}$$

Please cite this article in press as: F. Fang et al., Non-linear Petrov–Galerkin methods for reduced order hyperbolic equations and discontinuous finite element methods, J. Comput. Phys. (2012), http://dx.doi.org/10.1016/j.jcp.2012.10.011

in which the $\mathcal{M} \times \mathcal{M}$ diagonal matrix containing the diffusion coefficients is:

$$\mathbf{K} = \mathbf{V}(\mathbf{A}_{xt} \cdot \nabla_{xt}\Psi)\mathbf{P}^*_{xt}\mathbf{V}(\|\nabla_{xt}\Psi\|_2^2)^{-1}\mathbf{V}(\mathbf{r}). \tag{41}$$

The resulting diagonal matrix $\mathbf{K}$ can be modified to ensure non-negative diffusion by setting any of its negative entries to zero or taking their absolute values. Alternatively one can work with the residual only, by replacing $\mathbf{A}_{xt} \cdot \nabla_{xt}\Psi$ with the residual $\mathbf{r}$, which results in:

$$\mathbf{K} = \mathbf{V}(\mathbf{r})^T\mathbf{P}^*_{xt}\mathbf{V}(\|\nabla_{xt}\Psi\|_2^2)^{-1}\mathbf{V}(\mathbf{r}), \tag{42}$$

which is always positive because $\mathbf{P}^*_{xt}$ is positive semi-definite (as well as diagonal) and in which $\mathbf{V}(\mathbf{r})$ is the diagonal matrix containing the residual of the governing equations on its diagonal. Eq. (42) for the diffusivity can be derived by re-defining $\mathbf{A}^*_{xt}$ in Eq. (28) to:

$$\mathbf{A}^*_{xt} = \mathbf{V}(\mathbf{r})\mathbf{V}(\|\nabla_{xt}\Psi\|_2^2)^{-1}\nabla_{xt}\Psi. \tag{43}$$

3.2. Simplified coupled equations

Assuming time is discretised using the two level θ-method:

$$\mathbf{r} = \mathbf{A}_t\frac{\Psi^{n+1} - \Psi^n}{\Delta t} + \mathbf{A} \cdot \nabla\Psi^{n+\theta} - \mathbf{s}^{n+\theta}, \tag{44}$$

with $\mathbf{A} = (\mathbf{A}_x\ \mathbf{A}_y\ \mathbf{A}_z)^T$ and $\Psi^{n+\theta} = \Theta\Psi^{n+1} + (\mathbf{I} - \Theta)\Psi^n$ in which Θ is a diagonal matrix containing the time stepping parameters and also defining

$$\nabla_{xt}\Psi = \left(\frac{\Psi^{n+1} - \Psi^n}{\Delta t},\ (\nabla\Psi^{n+\theta})^T\right)^T. \tag{45}$$

Using this definition Eq. (45) enables the application of the formalism of space–time discretisation, developed here, for example:

$$\mathbf{A}^*_{xt} = (\mathbf{A}^{*T}_t, \mathbf{A}^{*T})^T = \mathbf{V}(\mathbf{A}_{xt} \cdot \nabla_{xt}\Psi)\mathbf{V}(\|\nabla_{xt}\Psi\|_2^2)^{-1}\nabla_{xt}\Psi, \tag{46}$$

and

$$\mathbf{P}^*_{xt} = min\left\{\mathbf{E}^{-1}, \left(\frac{1}{4}(\|\mathbf{J}^{-1}\mathbf{A}^*\|_2)\right)^{-1}\right\}. \tag{47}$$

By applying diffusion only in Cartesian space the stabilized discrete equations in diffusion form can be written:

$$\int_{V_E}\mathbf{N}_i\mathbf{r}dV - \int_{\Gamma_E}\mathbf{N}_i(\mathbf{n}\cdot\mathbf{A})^-(\Psi^{n+\theta} - \Psi^{n+\theta}_{bc})d\Gamma + \int_{V_E}(\nabla\mathbf{N}_i)^T\mathbf{K}\nabla\Psi^{n+1}dV = \mathbf{0}, \tag{48}$$

or in a form where we apply integration by parts once to the transport terms:

$$\begin{aligned}&\int_{V_E}\mathbf{N}_i\left(\mathbf{A}_t\frac{\Psi^{n+1} - \Psi^n}{\Delta t} - \mathbf{s}^{n+\theta}\right)dV - \int_{V_E}\nabla\cdot(\mathbf{N}_i\mathbf{A})\Psi^{n+\theta}dV + \int_{\Gamma_E}\mathbf{N}_i(\mathbf{n}\cdot\mathbf{A})^-\Psi^{n+\theta}_{bc} + \int_{\Gamma_E}\mathbf{N}_i(\mathbf{n}\cdot\mathbf{A})^+\Psi^{n+\theta}d\Gamma\\ &\quad + \int_{V_E}(\nabla\mathbf{N}_i)^T\mathbf{K}\nabla\Psi^{n+1}dV\\ &\quad = \mathbf{0}.\end{aligned} \tag{49}$$

4. Stable reduced order modelling using diffusion from Petrov–Galerkin methods

In this section, the Petrov–Galerkin method discussed above is applied to form conservative stablisation methods for ROM's which for non-linear problems have a tendency to diverge due to inadequate sub-grid-scale modelling (if Galerkin methods are applied e.g. the POD method).

4.1. Derivation of Petrov–Galerkin POD models

If the original discrete system at a given time level is

$$\mathbf{A}\Psi = \mathbf{b}, \tag{50}$$

Please cite this article in press as: F. Fang et al., Non-linear Petrov–Galerkin methods for reduced order hyperbolic equations and discontinuous finite element methods, J. Comput. Phys. (2012), http://dx.doi.org/10.1016/j.jcp.2012.10.011

its modified discrete system is then written:

$$\mathbf{C}^T\mathbf{W}^{-1}\mathbf{A}\Psi = \mathbf{C}^T\mathbf{W}^{-1}\mathbf{b}, \tag{51}$$

in which for least squares, $\mathbf{C} = \mathbf{A}$. Note that the solution of this Eq. (51) is the same as the original system (50) however critically, it is not so when the reduced order modelling is applied. The weighting matrix $\mathbf{W}$ can be chosen such as to render the system of equations dimensionally consistent (and thus may contain characteristic dimensions such as the time step size Δt and a length scale) and also contain the mass matrix of the system. Least squares (LS) methods [17] have dissipative properties, unlike Galerkin methods, but are not generally conservative for coupled systems of equations. However LS methods may be applied at each equation level to make them conservative, in which case $\mathbf{C}$ may contain just parts of the matrix $\mathbf{A}$.

Using POD methods any variable ψ can be approximately expressed as an expansion of the first few POD basis functions $\{\phi_1, \ldots, \phi_M\}$:

$$\psi(\mathbf{x}, t) = \bar{\psi}(\mathbf{x}) + \sum_{m=1}^{M} \alpha_m(t)\phi_m(\mathbf{x}), \tag{52}$$

where $\bar{\psi}$ is the mean of the variables ψ over the time, α_m $(1 \leqslant m \leqslant M)$ are the time-dependent coefficients to be determined.

In FE method, the variable ψ can be expressed as:

$$\psi_m = \sum_{j=1}^{\mathcal{N}} N_{xtj}\Psi_{mj}, \tag{53}$$

and the POD basis functions:

$$\phi_m = \sum_{j=1}^{\mathcal{N}} N_{xtj}\Phi_{mj}. \tag{54}$$

Thus, taking into account (52), the variables $\Psi = (\Psi_1, \ldots, \Psi_{\mathcal{N}})$ can be written:

$$\Psi = \overline{\Psi} + \mathbf{M}^{POD}\Psi^{POD}, \tag{55}$$

where $\Psi^{POD} = (\alpha_1, \ldots, \alpha_M)^T$, and the matrix $\mathbf{M}^{POD}$ which consists of the POD basis functions, *i.e.* $\mathbf{M}^{POD} = [\Phi_1, \ldots, \Phi_M] \in R^{\mathcal{N}\times M}$, in which $\Phi_m = (\Phi_{m1}, \ldots, \Phi_{m\mathcal{N}})^T$ $(1 \leqslant m \leqslant M)$.

The reduced order model can be obtained by projecting the original models onto the reduced space, *i.e.* in a method analogous to the Galerkin method, taking the POD basis function as the test function, then integrating it over the computational domain Ω. By multiplying (50) by the matrix $\mathbf{M}^{POD^T}$ and taking into account (55), the POD discrete model of (50) is obtained:

$$\mathbf{M}^{POD^T}\mathbf{A}\mathbf{M}^{POD}\Psi^{POD} = \mathbf{M}^{POD^T}(\mathbf{b} - \mathbf{A}\overline{\Psi}). \tag{56}$$

For the LS method (see (51)), Eq. (56) is:

$$\mathbf{M}^{POD^T}\mathbf{C}^T\mathbf{W}^{-1}\mathbf{A}\mathbf{M}^{POD}\Psi^{POD} = \mathbf{M}^{POD^T}\mathbf{C}^T\mathbf{W}^{-1}(\mathbf{b} - \mathbf{A}\overline{\Psi}). \tag{57}$$

Using the non-linear Petrov–Galerkin mechanics discussed in Section 3, the POD reduced order model can thus be written:

$$\mathbf{M}^{POD^T}(\mathbf{I} + \mathbf{C}^T\mathbf{W}^{-1})\mathbf{A}\mathbf{M}^{POD}\Psi^{POD} = \mathbf{M}^{POD^T}(\mathbf{I} + \mathbf{C}^T\mathbf{W}^{-1})(\mathbf{b} - \mathbf{A}\overline{\Psi}), \tag{58}$$

or in diffusion form (analogous to (39)–(41)):

$$(\mathbf{M}^{POD^T}\mathbf{A}\mathbf{M}^{POD} + \mathbf{K})\Psi^{POD} = \mathbf{M}^{POD^T}(\mathbf{b} - \mathbf{A}\overline{\Psi}), \tag{59}$$

where the calculation of the diffusion matrix $\mathbf{K}$ will be discussed below in Sections 4.2 and 5. As we know, a common solution to the divergence of ROM solutions (56) is to add diffusion terms into the equations and tune these diffusion terms to a best match the full model solution. The nonlinear Petrov–Galerkin POD method (59) presents a natural and easy way to introduce a diffusion term into ROM without tuning/optimising and provides appropriate modelling and stabilisations for the numerical solution of high order nonlinear PDEs.

4.2. Calculation of the diffusion coefficient

Reminding that the construction of the POD model is similar to that of the Galerkin FE model, the diffusion coefficient in $\mathbf{K}$ can thus be calculated (analogous to (17)):

$$\nu^{POD} = \frac{r^{POD}p_{xt}^{*^{POD}}r^{POD}}{\|\nabla_{xt}\psi^{POD}\|_2^2}, \tag{60}$$

Please cite this article in press as: F. Fang et al., Non-linear Petrov–Galerkin methods for reduced order hyperbolic equations and discontinuous finite element methods, J. Comput. Phys. (2012), http://dx.doi.org/10.1016/j.jcp.2012.10.011

where

$$p_{xt}^{*^{POD}} = \beta min_k \left\{ \frac{1}{4} \left(\left| \frac{\mathbf{a}_{xt}^* \cdot \nabla_{xt} N_{xt_k}^{POD}}{max_{\mathbf{x}}\{|N_{xt_k}^{POD}(\mathbf{x})|\}} \right| \right)^{-1} \right\}, \tag{61}$$

in which we have assumed that the length scale associated with the POD method is the gradient of the normalised POD basis function in the direction $\mathbf{a}_{xt}^*$, and β is a scalar. Theoretically, β can vary between 0 and 1. When $\beta = 1$, the Petrov–Galerkin approach is fully applied to the POD model, while the Galerkin POD is used when $\beta = 0$. Thus, any value $\beta \in [0, 1]$ is a reasonable choice with less dissipation introduced for smaller values of beta. We choose a large value of β when the POD numerical simulation becomes unstable which usually happens when a small number of POD bases are used (e.g. results shown in Fig. 5, where only 10 POD bases are chosen).

The residual vector can be determined from:

$$\mathbf{r}^{POD} = \mathbf{E}^{POD^{-1}}((\mathbf{M}^{POD^T}\mathbf{A}\mathbf{M}^{POD})\Psi^{POD} - \mathbf{M}^{POD^T}(\mathbf{b} - \mathbf{A}\overline{\Psi})), \tag{62}$$

where $\mathbf{E}_{ij}^{POD} = \int_V \Psi_i^{POD}\Psi_j^{POD}\,dV$, taking into account the ROM basis functions are orthonormal, so $\mathbf{E}^{POD} = \mathbf{I}$. Since the absolute value of the residual may not matter:

$$\mathbf{r}^{POD} = \mathbf{E}^{POD^{-1}}\mathbf{M}^{POD^T}|\mathbf{A}\mathbf{M}^{POD}\Psi^{POD} - (\mathbf{b} - \mathbf{A}\overline{\Psi})|, \tag{63}$$

To avoid the integration over the domain, there is another approach to calculate the coefficient of the diffusion term. Since the POD matrices may be relatively small one can manipulate their eigen structure in order to construct stabilization methods. Assuming v^{POD} is represented using a POD expansion ($v^{POD} = \sum_{k=1}^{M} N_k^{POD} v_k^{POD}$), the vector $\underline{v}^{POD} = (v_1^{POD}, \ldots, v_M^{POD})$ is thus written (see details in Appendix A):

$$\underline{v}^{POD} = |\mathbf{O}^{POD^{-1}}\mathbf{U}^{POD^{-1}}\mathbf{q}|, \tag{64}$$

where

$$\mathbf{U}_{mk}^{POD} = \int_V N_{xt_m}^{POD}\left(\left(\frac{\partial\psi}{\partial t}\right)^2 + \left(\frac{\partial\psi}{\partial x}\right)^2 + \left(\frac{\partial\psi}{\partial y}\right)^2 + \left(\frac{\partial\psi}{\partial z}\right)^2 + \epsilon\right)N_{xt_k}^{POD}\,dV, \tag{65}$$

in which the small scalar ϵ ensures that $\mathbf{U}$ is non-singular. The residual term $q = r^{POD}r^{POD}$ cab be expressed as the expansion of POD basis functions:

$$q = r^{POD}r^{POD} = \sum_{k=1}^{M} N_{xt_k}^{POD} q_k, \tag{66}$$

with $\mathbf{q} = (q_1\ q_2\ \ldots\ q_{\mathcal{N}^{POD}})^T$. Multiplying (66) by $N_{xt_m}^{POD}$ and integrating it over the domain, yields

$$\int_V N_{xt_m}^{POD} q\,dV = \int_V N_{xt_m}^{POD} r^{POD} r^{POD}\,dV = \int_V N_{xt_m}^{POD} \sum_{k=1}^{M} N_{xt_k}^{POD} q_k. \tag{67}$$

Taking into account the orthonormal property of POD the mth equation of Eq. (67) becomes:

$$q_m = \int_V N_{xtm}^{POD} r^{POD} r^{POD}\,dV. \tag{68}$$

For calculation of $\mathbf{O}^{POD^{-1}}$ in (64), we define a matrix $\mathbf{B}$:

$$(\mathbf{B}\Psi)_i = \sum_{V_E}\left(\int_{V_E} \mathbf{N}_{xti}\mathbf{A}_{xt}^* \cdot \nabla_{xt}\Psi\,dV - \int_{\Gamma_E} \mathbf{N}_{xti}(\mathbf{n}_{xt} \cdot \mathbf{A}_{xt})^-(\Psi - \Psi_{bc})d\Gamma\right). \tag{69}$$

The matrix $\mathbf{B}^{POD}$ is then written:

$$\mathbf{B}^{POD} = \mathbf{M}^{POD^T}\mathbf{B}\mathbf{M}^{POD}. \tag{70}$$

Using the eigen-decomposition $\mathbf{B}^{POD} = \mathbf{L}_B^{POD}\mathbf{\Lambda}_B^{POD}\mathbf{R}_B^{POD}$ the matrix $\mathbf{O}^{POD^{-1}}$ in (64) can be thus written:

$$\mathbf{O}^{POD^{-1}} = \beta\frac{1}{4}\mathbf{R}_{B^{POD}}|\mathbf{\Lambda}_{B^{POD}}|^{-1}\mathbf{L}_{B^{POD}}. \tag{71}$$

An alternative definition to $\mathbf{O}^{POD^{-1}}$ defined by Eq. (71) is:

$$\mathbf{O}^{POD^{-1}} = \beta\frac{1}{4}|\mathbf{B}^{POD^T}\mathbf{B}^{POD}|^{-\frac{1}{2}} = \beta\frac{1}{4}\mathbf{L}_{B^{POD^T}B^{POD}}|\mathbf{\Lambda}_{B^{POD^T}B^{POD}}|^{-\frac{1}{2}}\mathbf{R}_{B^{POD^T}B^{POD}}. \tag{72}$$

Thus $|\mathbf{\Lambda}_{B^{POD^T}B^{POD}}|^{-\frac{1}{2}}$ should have similar values to p_{xt}^* calculated from Eq. (61). A good choice suggested by the non-linear Petrov–Galerkin approach for $\mathbf{C}$ in Eq. (58) is $\mathbf{C} = \mathbf{B}$ which is very similar to the diffusion based method.

Please cite this article in press as: F. Fang et al., Non-linear Petrov–Galerkin methods for reduced order hyperbolic equations and discontinuous finite element methods, J. Comput. Phys. (2012), http://dx.doi.org/10.1016/j.jcp.2012.10.011

5. Bassi Rebay representation of DG diffusion

One of the key ingredients of DG methods is the formulation of interface (numerical) fluxes, which provide a weak coupling between the unknowns in neighbouring elements. The classic approach introduced by Bassi and Rebay in 1997 [8] is here used for the representation of the DG diffusion term. The diffusion term is written:

$$\sum_{ele}\int_{V_E} N_i \frac{\partial}{\partial x} v \frac{\partial \psi}{\partial x} dV_E = -\sum_{ele}\int_{V_E} v \frac{\partial N_i}{\partial x}\frac{\partial \psi}{\partial x} dV_E + \sum_{ele}\int_{\Gamma_E} v N_i \mathbf{n_x}\cdot\frac{\partial \psi}{\partial \mathbf{x}} \mathbf{d}\Gamma_\mathbf{E}. \tag{73}$$

Defining

$$\psi_x = \frac{\partial \psi}{\partial x}, \tag{74}$$

the diffusion term (73) can be rewritten:

$$\begin{aligned}\sum_{ele}\int_{V_E} \frac{\partial}{\partial x} v N_i \frac{\partial \psi}{\partial x} dV_E &= -\sum_{ele}\int_{V_E} v \frac{\partial N_i}{\partial x}\psi_x dV_E + \sum_{ele}\int_{\Gamma_E} v N_i \mathbf{n_x}\cdot\psi_\mathbf{x}\mathbf{d}\Gamma_\mathbf{E} \\ &= -\sum_{\mathbf{ele}}\int_{\mathbf{V_E}} v \frac{\partial \mathbf{N_i}}{\partial \mathbf{x}}\psi_\mathbf{x}\mathbf{dV_E} + \sum_{\mathbf{ele}}\int_{\Gamma_\mathbf{E}} v\mathbf{N_i}\,\mathbf{n_x}\cdot\frac{\mathbf{1}}{\mathbf{2}}(\psi_{\mathbf{xcur}}+\psi_{\mathbf{xnei}})\mathbf{d}\Gamma_\mathbf{E} = \mathbf{C^T}\boldsymbol{\psi}_\mathbf{x},\end{aligned} \tag{75}$$

where ψ_{xcur} and ψ_{xnei} represent ψ_x at the current and neighbouring elements, respectively, and ψ_x is zero on the boundary, *i.e.* zero through the surface integral. Multiplying (74) by N_i and integrating it over the domain V, obtains

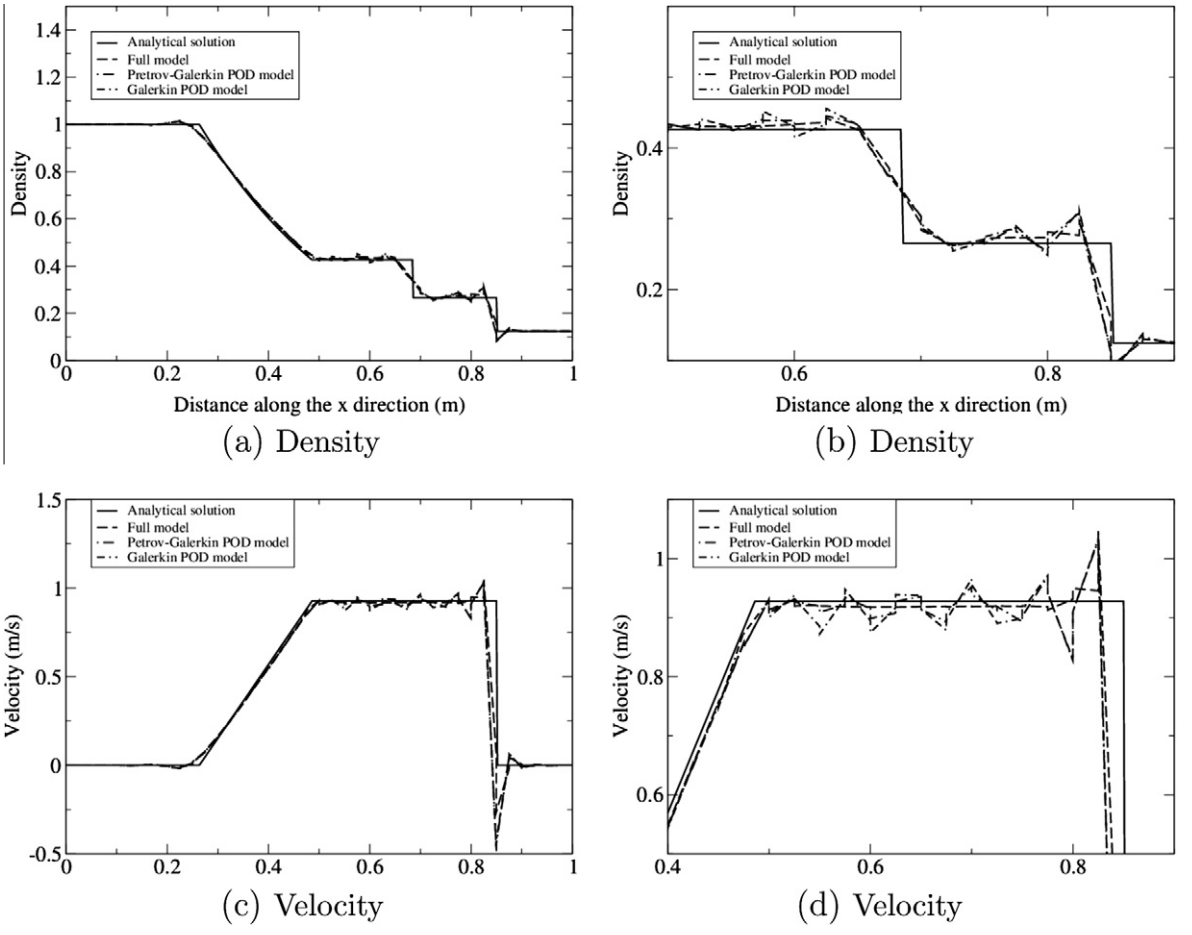

Fig. 1. Case 1 (the Sod shock tube problem): comparison of the results obtained from the POD and full model at time level $t = 0.2$ s (where 15 POD bases are used to represent 95% of the original energy).

$$\begin{aligned}\sum_{ele}\int_{V_E} N_i\psi_x dV_E &= \sum_{ele}\int_{V_E} N_i\frac{\partial\psi}{\partial x}dV_E = -\sum_{ele}\int_{V_E}\frac{\partial N_i}{\partial x}\psi dV_E + \sum_{ele}\int_{\Gamma_E} N_i\,\mathbf{n_x}\cdot\psi\mathbf{d\Gamma_E}\\ &= -\sum_{\mathbf{ele}}\int_{\mathbf{V_E}}\frac{\partial \mathbf{N_i}}{\partial \mathbf{x}}\psi\mathbf{dV_E} + \sum_{\mathbf{ele}}\int_{\mathbf{\Gamma_E}}\mathbf{N_i}\,\mathbf{n_x}\cdot\frac{\mathbf{1}}{\mathbf{2}}(\psi_{\mathbf{cur}}+\psi_{\mathbf{nei}})\mathbf{d\Gamma_E}\\ &= \sum_{\mathbf{ele}}\int_{\mathbf{V_E}}\mathbf{N_i}\frac{\partial\psi}{\partial\mathbf{x}}\mathbf{dV_E} - \sum_{\mathbf{ele}}\int_{\mathbf{\Gamma_E}}\mathbf{N_i}\,\mathbf{n_x}\cdot\psi_{\mathbf{cur}}\mathbf{d\Gamma_E} + \sum_{\mathbf{ele}}\int_{\mathbf{\Gamma_E}}\mathbf{N_i}\,\mathbf{n_x}\cdot\frac{\mathbf{1}}{\mathbf{2}}(\psi_{\mathbf{cur}}+\psi_{\mathbf{nei}})\mathbf{d\Gamma_E}\\ &= \sum_{\mathbf{ele}}\int_{\mathbf{V_E}}\mathbf{N_i}\frac{\partial\psi}{\partial\mathbf{x}}\mathbf{dV_E} - \sum_{\mathbf{ele}}\int_{\mathbf{\Gamma_E}}\mathbf{N_i}\,\mathbf{n_x}\cdot\frac{\mathbf{1}}{\mathbf{2}}(\psi_{\mathbf{cur}}-\psi_{\mathbf{nei}})\mathbf{d\Gamma_E} = \mathbf{F\Psi},\end{aligned} \tag{76}$$

where ψ_{cur} and ψ_{nei} represent ψ at the current and neighbouring elements respectively. Eq. (76) can be rewritten:

$$\mathbf{M}\boldsymbol{\psi}_\mathbf{x} = \mathbf{F\Psi}, \tag{77}$$

where $\mathbf{M}$ is the mass matrix in FE, and $\psi_x = \frac{\partial\psi}{\partial x}$ can be calculated:

$$\boldsymbol{\psi}_\mathbf{x} = \mathbf{M}^{-1}\mathbf{F\Psi}. \tag{78}$$

The diffusion term (75) can be-rewritten:

$$\sum_{ele}\int_{V_E} N_i\frac{\partial}{\partial x}v\frac{\partial\psi}{\partial x}dV_E = \mathbf{C}^T\mathbf{M}^{-1}\mathbf{F\Psi}. \tag{79}$$

The approach discussed above is easily extended to 2D and 3D cases.

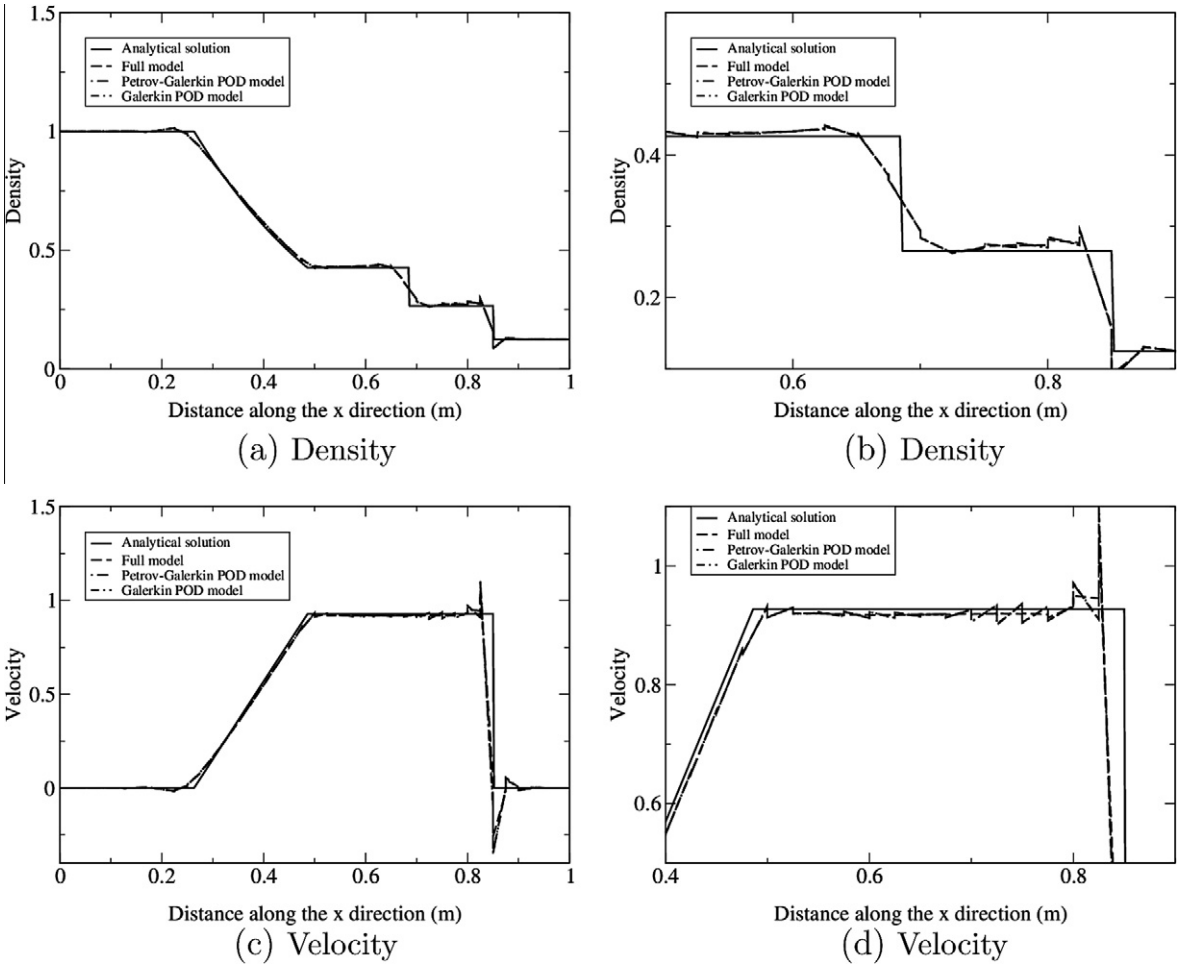

Fig. 2. Case 1 (the Sod shock tube problem): Comparison of the results obtained from the POD and full model at time level $t = 0.2$ s (where 25 POD bases are used to represent 99.4% of the original energy).

Please cite this article in press as: F. Fang et al., Non-linear Petrov–Galerkin methods for reduced order hyperbolic equations and discontinuous finite element methods, J. Comput. Phys. (2012), http://dx.doi.org/10.1016/j.jcp.2012.10.011

6. Example cases: advection and shock waves

Shock waves are characterised by an abrupt, discontinuous change in the characteristics of the medium. The shock waves are described by the nonlinear hyperbolic Euler equations in a non-conservation form:

$$\frac{\partial \psi}{\partial t} + a_x \frac{\partial \psi}{\partial x} = 0. \tag{80}$$

In this work, the Petrov–Galerkin POD method discussed above is applied to (80). A diffusional DG is used to control numerical oscillations. The root mean square error (RMSE), relative error (RE) and correlation coefficient of results between the POD and full models at the time level n is used to estimate the error of the POD/ROM projection results:

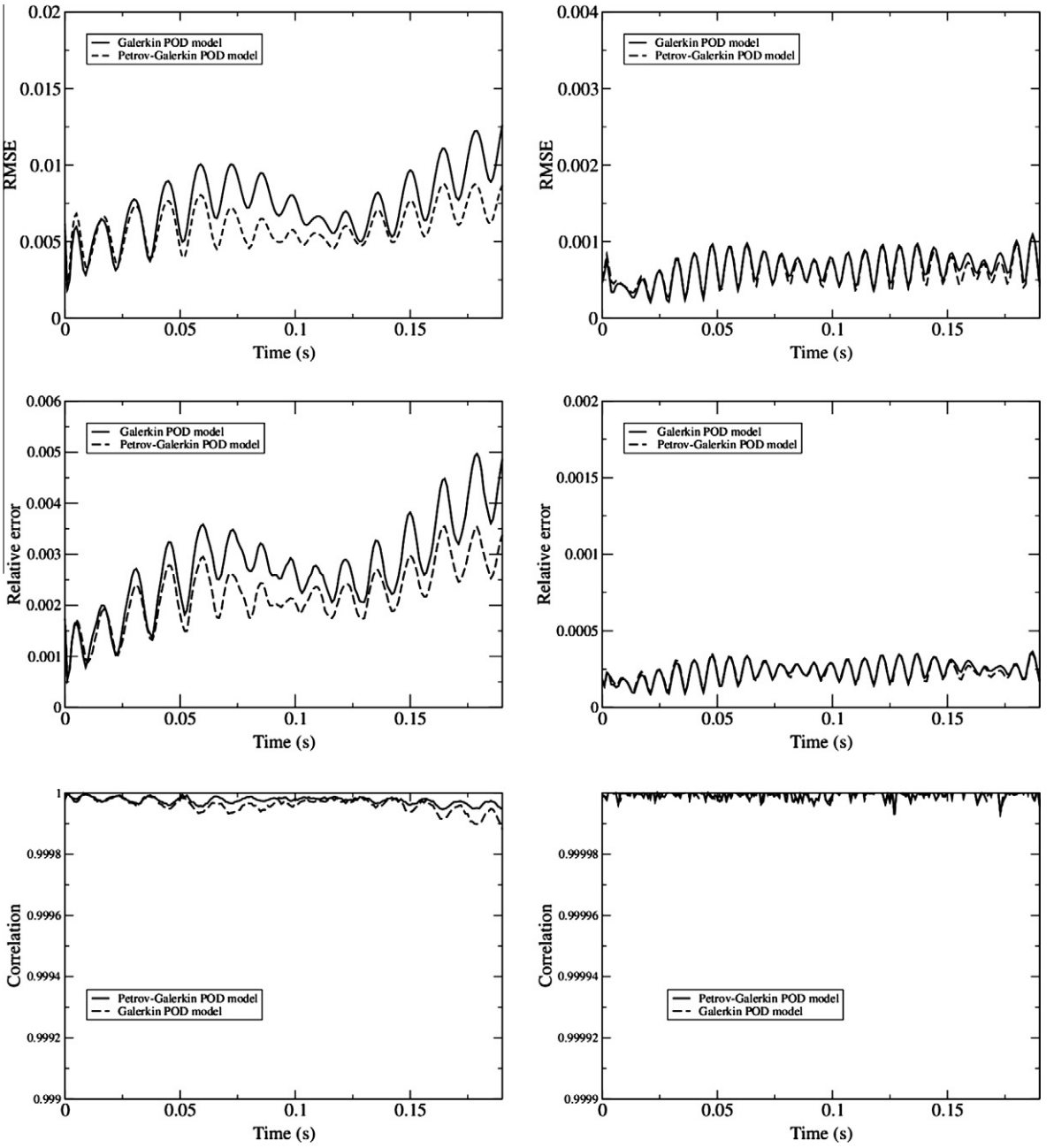

Fig. 3. Case 1 (the Sod shock tube problem): RMSE of results between the POD model and the full model (left panel: 15 POD bases which are used to represent 95% of the original energy; right panel: 25 POD bases which are used represent 99.4% of the original energy).

Please cite this article in press as: F. Fang et al., Non-linear Petrov–Galerkin methods for reduced order hyperbolic equations and discontinuous finite element methods, J. Comput. Phys. (2012), http://dx.doi.org/10.1016/j.jcp.2012.10.011

$$RMSE^n = \sqrt{\frac{\sum_{i=1}^{\mathcal{N}} (\psi_i^n - \psi_{o,i}^n)^2}{\mathcal{N}}}, \tag{81}$$

where ψ_i^n and $\psi_{o,i}^n$ are the vectors containing the POD and full model results at the node i respectively, and relative error is calculated:

$$RE^n = \frac{\sum_{i=1}^{\mathcal{N}} (\psi_i^n - \psi_{o,i}^n)^2}{\sum_{i=1}^{\mathcal{N}} \psi_i^n}. \tag{82}$$

The correlation coefficient of results between the POD and full models at the time level n with expected values μ_{ψ^n} and $\mu_{\psi_o^n}$ and standard deviations σ_{ψ^n} and $\sigma_{\psi_o^n}$ is defined as:

$$corr(\psi^n, \psi_o^n)^n = \frac{cov(\psi^n, \psi_o^n)}{\sigma_{\psi^n}\sigma_{\psi_o^n}} = \frac{E[(\psi^n - \sigma_{\psi^n})(\psi_o^n - \sigma_{\psi_o^n})]}{\sigma_{\psi^n}\sigma_{\psi_o^n}}. \tag{83}$$

6.1. Test case 1: the Sod shock tube problem

The Petrov–Galerkin POD model is validated in the classic Sod shock tube problem [21]. The POD model results are compared with the analytical solution [21] and those from the full model. The problem solved here has a unit 1D domain and open boundary conditions at both ends and space and time steps of $\Delta t = 0.001,\ \Delta x = 0.0238$. The simulation period is $[0, 0.2]$. The Euler Eq. (80) can be re-written for an ideal gas [22,18]:

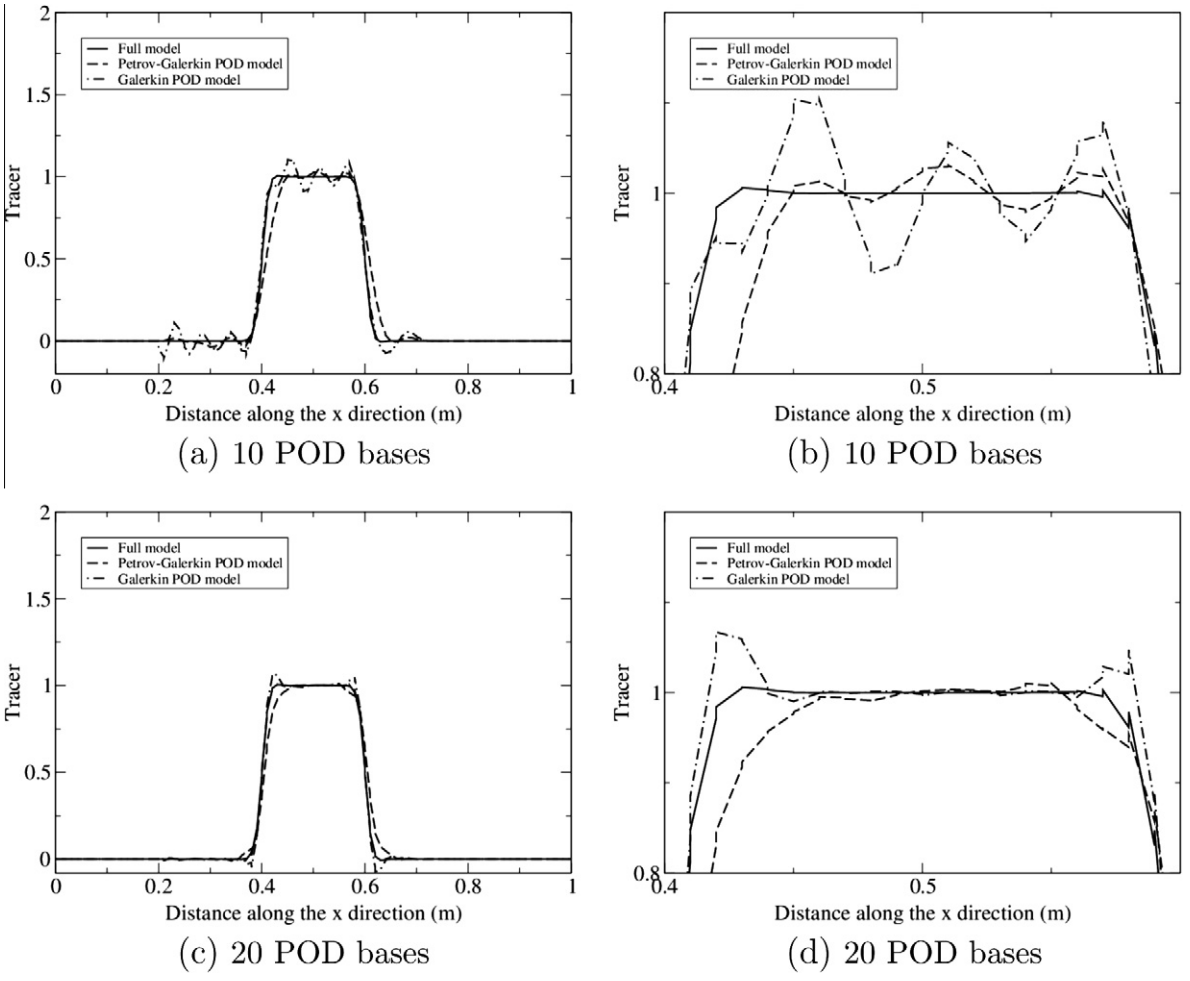

Fig. 4. Case 2 (1D advection): Comparison of the results between the full and POD models. Top panel: 10 POD bases which represent 88% of the original energy; bottom panel: 20 POD bases which represent 99% of the original energy. The first approach (60) is used ($\beta = 1.0$) and the mesh size: $\Delta x = 0.01$ m.

Please cite this article in press as: F. Fang et al., Non-linear Petrov–Galerkin methods for reduced order hyperbolic equations and discontinuous finite element methods, J. Comput. Phys. (2012), http://dx.doi.org/10.1016/j.jcp.2012.10.011

$$\begin{pmatrix} \rho \\ \rho u \\ e \end{pmatrix}_t + \begin{pmatrix} \rho u \\ \rho u^2 + p \\ u(e+p) \end{pmatrix}_x = \begin{pmatrix} 0 \\ 0 \\ 0 \end{pmatrix}, \tag{84}$$

or in a matrix form, $\mathbf{A}_{xt}\Psi = 0$, where

$$\mathbf{A}_t = \mathbf{I}, \tag{85}$$

$$\mathbf{A}_x = \begin{pmatrix} 0 & 1 & 0 \\ \frac{\gamma-3}{2}u^2 & (3-\gamma)u & \gamma - 1 \\ \gamma u e + (\gamma-1)u^3 & \gamma e - \frac{2}{3}(\gamma-1)u^2 & \gamma u \end{pmatrix}, \tag{86}$$

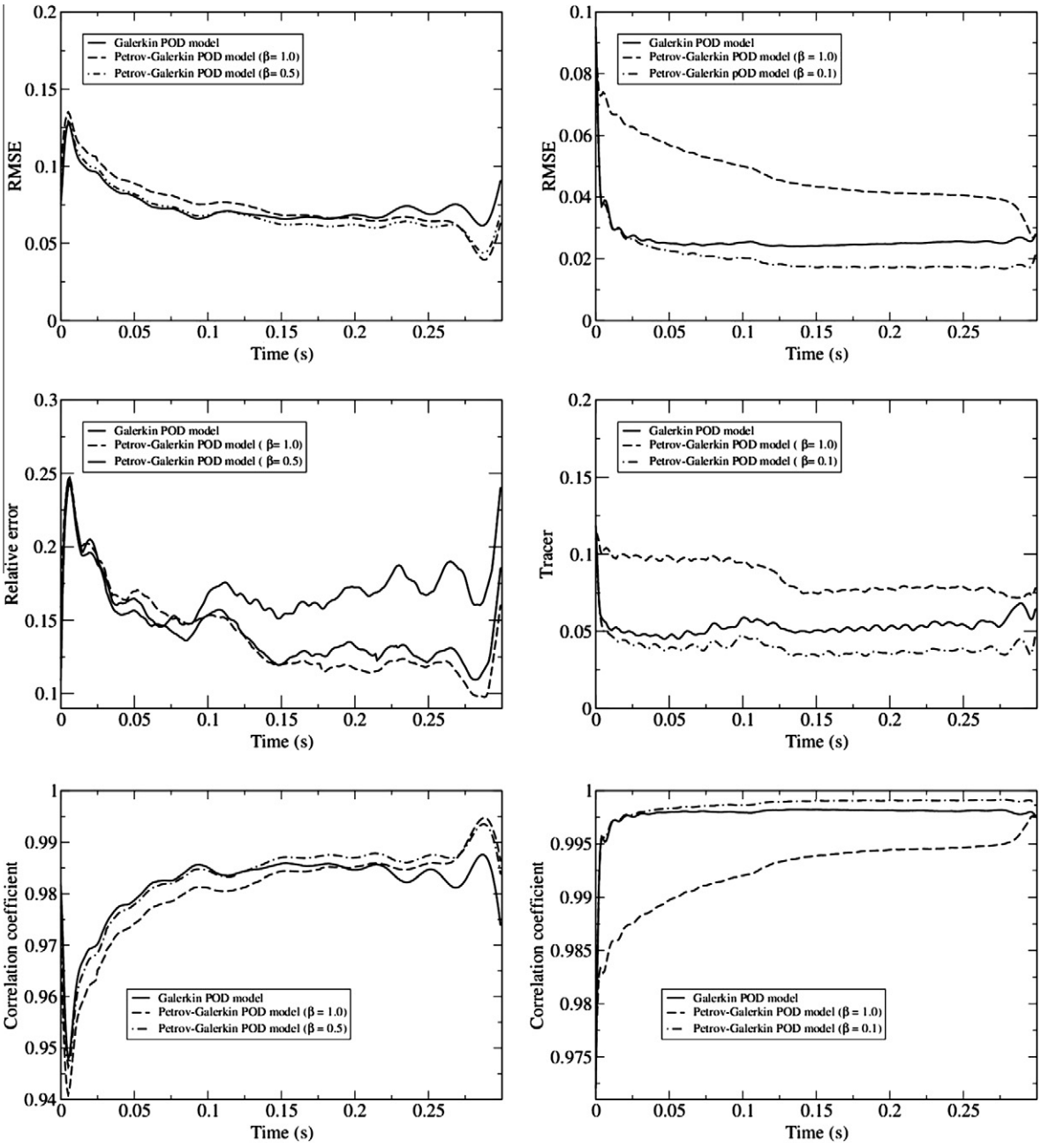

Fig. 5. Case 2 (1D advection): RMSE and correlation coefficient of results between the POD and full models (left: 10 POD bases are used to represent 88% of the original energy; right: 20 POD bases are used to represent 99% of the original energy; where β is the scalar in (60)).

Please cite this article in press as: F. Fang et al., Non-linear Petrov–Galerkin methods for reduced order hyperbolic equations and discontinuous finite element methods, J. Comput. Phys. (2012), http://dx.doi.org/10.1016/j.jcp.2012.10.011

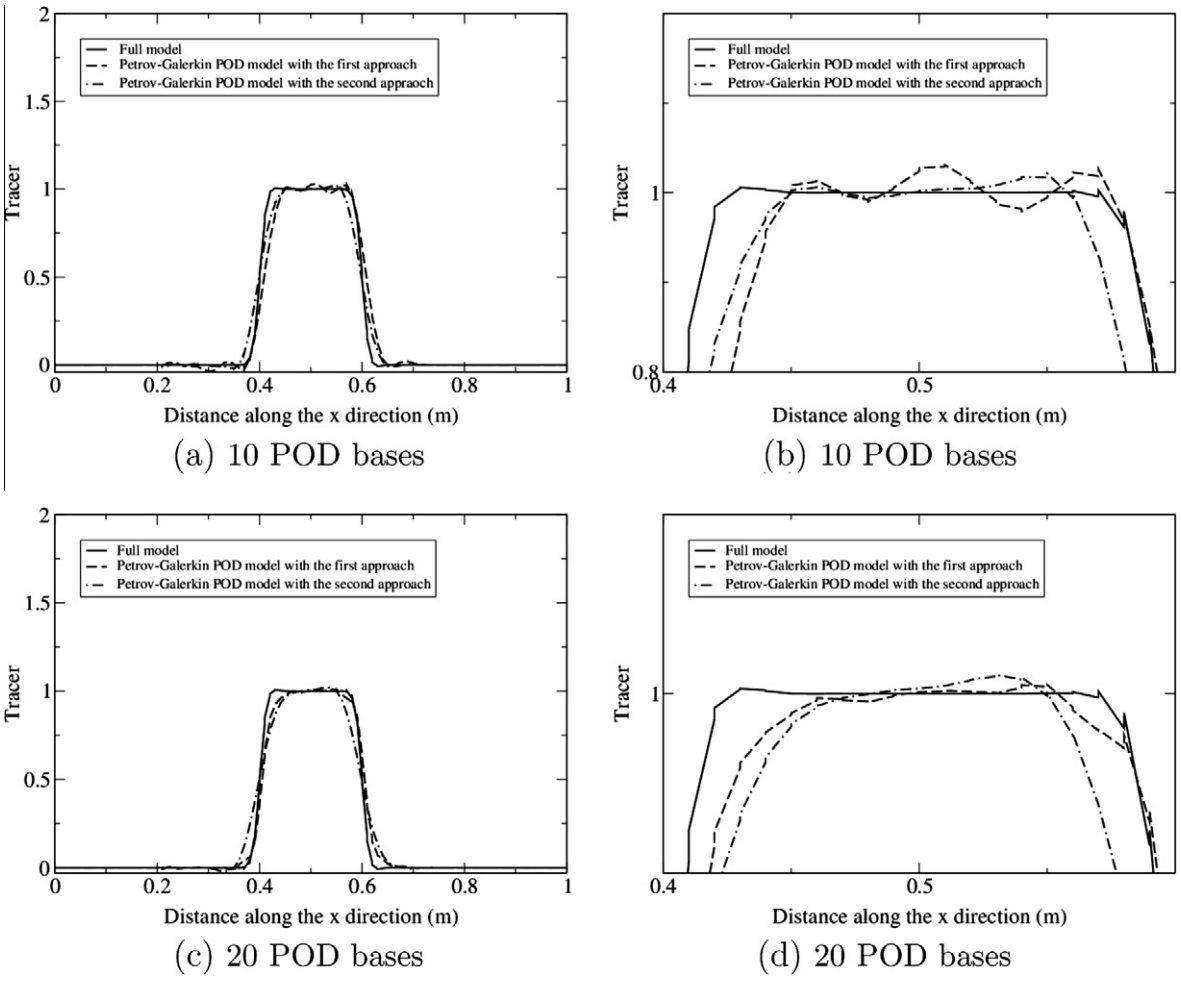

Fig. 6. Case 2 (1D advection): comparison of results obtained from the Petrov–Galerkin POD model using: the first approach (60) ($\beta = 1.0$); and the second approach (64) ($\beta = 0.01$) used with (72). The mesh size: $\Delta x = 0.01$ m.

where ρ is the density of the fluid, u is the fluid velocity, e is the energy per unit volume (length), and p is the pressure. The equation of state is

$$p = (\gamma - 1)\left(e - \frac{1}{2}\rho u^2\right), \tag{87}$$

where γ is the adiabatic gas index. For an ideal gas $\gamma = 1.4$. The test consists of a 1D Riemann problem with the following parameters, for left and right states of an ideal gas:

$$\begin{pmatrix} \rho_L \\ p_L \\ u_L \end{pmatrix} = \begin{pmatrix} 1.0 \\ 1.0 \\ 0.0 \end{pmatrix}, \begin{pmatrix} \rho_R \\ p_R \\ u_R \end{pmatrix} = \begin{pmatrix} 0.125 \\ 0.1 \\ 0.0 \end{pmatrix}. \tag{88}$$

Linear elements are used in space and time. The value of $\mathbf{A}_{\mathbf{xt}}$ in the boundary element integral is calculated by the Roe average approach (see Eq. (48)) [27].

The results from the POD and full models are provided in Figs. 1, and 2. It is shown that the Petrov–Galerkin POD model does well in capturing and resolving discontinuities of shock waves. The results reproduce the correct density and velocity profiles of the rarefaction wave. When 15 POD bases are used (where 95% of the original energy is captured), the RMSE of results between the Petrov–Galerkin POD and full models is less than 0.0075 (while less than 0.035 for the relative error) and is further reduced to 0.001 (0.0045 for the relative error) with 25 POD bases (where 99.4% of the original energy is represented) (see Fig. 3). The correlation coefficient of results achieves a value of 99.99%.

Please cite this article in press as: F. Fang et al., Non-linear Petrov–Galerkin methods for reduced order hyperbolic equations and discontinuous finite element methods, J. Comput. Phys. (2012), http://dx.doi.org/10.1016/j.jcp.2012.10.011

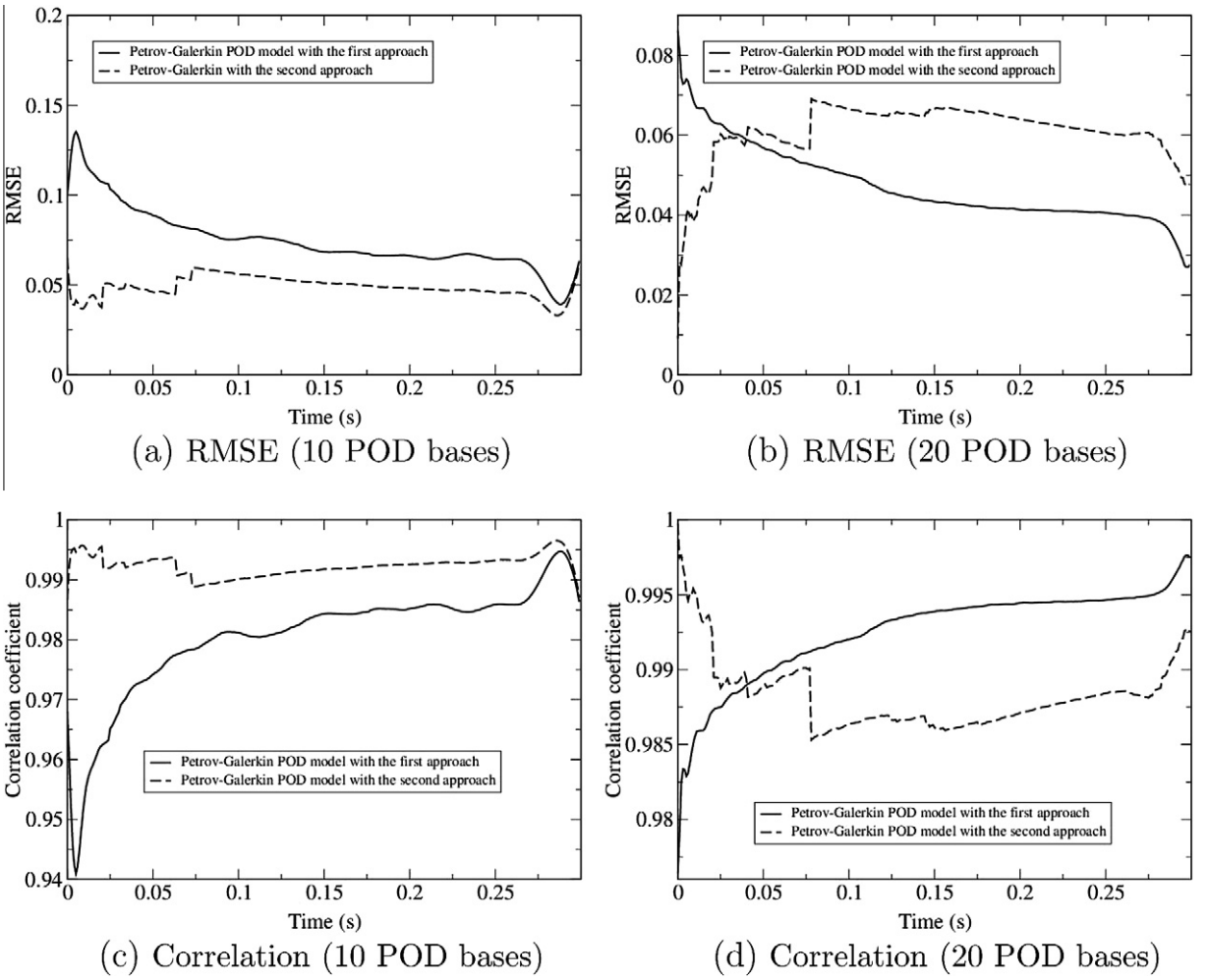

Fig. 7. Case 2 (1D advection): RMSE and correlation coefficient of results between the full and Petrov–Galerkin POD models using: the first approach (60) ($\beta = 1.0$); and the second approach (64) ($\beta = 0.01$) used with (72). The mesh size: $\Delta x = 0.01$ m.

6.2. Test case 2: 1D advection

The problem solved here has a unit 1D domain and open boundary conditions at both ends and space and time steps of $\Delta t = 0.001$, $\Delta x = 0.005$ respectively. The simulation period is $[0, 0.2]$. Linear elements are used in space and time. The initial condition is

$$\psi_{t=0} = \begin{cases} 1.0 & 0.2 < x < 0.4; \\ 0.0 & x \leqslant 0.2;\ x \geqslant 0.4. \end{cases}$$

Fig. 4 shows the comparison of the results between the full and POD models. It is observed that the instability in the POD results is reduced by using the Petrov–Galerkin POD methods (Fig. 4). The RMSE, relative error and correlation coefficient of results between the POD and full models during the simulation period are provided in Fig. 5. It can be seen that by using the Petrov–Galerkin POD model, the RMSE of results between the POD and full models is reduced up to 20% of that of the Galerkin POD modelling at the end of the simulation period. The correlation coefficient of results exceeds 98% when the Petrov–Galerkin method is used. With an increase in the number of POD bases (where 99% of the original energy can be captured with 20 POD bases while 88% of the original energy with 10 POD bases), the RMSE of POD results using the Petrov–Galerkin method is further reduced and attains a small value (less than 0.02) while the correlation coefficient achieves 99.9%. By choosing a suitable scalar β for the calculation of the diffusion coefficient, the RMSE of POD results can be also decreased. The relative error of results between the full and POD models can be decreased by half of that of the Galerkin POD modelling (see Fig. 5(c)) with 10 POD bases and less than 0.05 when 20 POD bases are used. The scalar diffusion coefficient used in the Petrov–Galerkin POD model can be calculated by either (60) or (64) and the corresponding results are shown in Figs. 6 and 7. The Petrov–Galerkin POD results using Eq. (64) are much smoother than those with the use of (60).

Please cite this article in press as: F. Fang et al., Non-linear Petrov–Galerkin methods for reduced order hyperbolic equations and discontinuous finite element methods, J. Comput. Phys. (2012), http://dx.doi.org/10.1016/j.jcp.2012.10.011

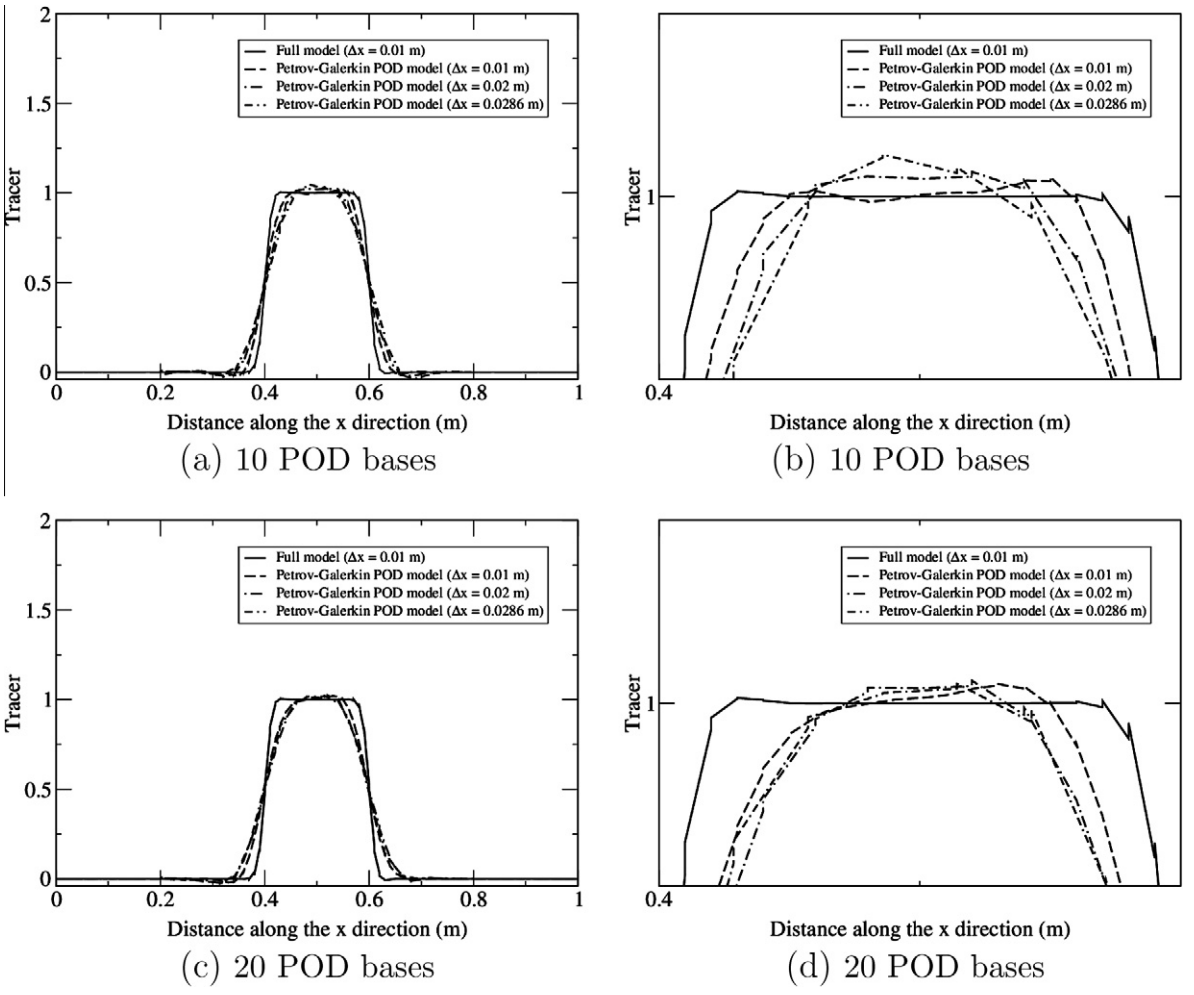

Fig. 8. Case 2 (1D advection): comparison of results obtained from the Petrov–Galerkin POD model based on different mesh resolution (using the second approach (64) ($\beta = 0.01$) used with (72).

A mesh refinement study has been carried out in this test case. The POD model is obtained on different resolution meshes, here, three mesh sizes are chosen ($\Delta x = 0.01, 0.02$ and 0.0286 m). Effect of mesh resolution on POD solutions is shown in Fig. 8. It can be seen that the POD model based on a higher resolution mesh provides more accurate results.

The Petrov–Galerkin POD model is also applied to Eq. (80) with the initial condition:

$$\psi_{t=0} = e^{-\frac{(x-0.3)^2}{0.1^2}}. \tag{89}$$

The results from the POD model exhibit an overall good agreement with those obtained with the full model (Fig. 9) with 5 POD bases.

6.3. Test case 3: 2D advection

The Petrov–Galerkin POD model in conjunction with the Bassi–Rebay approach is further applied to a 2D advection case. The problem solved here has a unit square domain with open boundary conditions and space and time steps of $\Delta t = 0.001,\ \Delta x = \Delta y = 0.01$. The simulation period is $[0, 0.2]$. Linear elements are used in space and time. The initial condition is

$$\psi_{t=0} = 1.0\sqrt{(x-0.5)^2 + (y-0.5)^2} \leqslant 0.05;$$

$$\psi_{t=0} = 0.0\sqrt{(x-0.5)^2 + (y-0.5)^2} > 0.05. \tag{90}$$

Please cite this article in press as: F. Fang et al., Non-linear Petrov–Galerkin methods for reduced order hyperbolic equations and discontinuous finite element methods, J. Comput. Phys. (2012), http://dx.doi.org/10.1016/j.jcp.2012.10.011

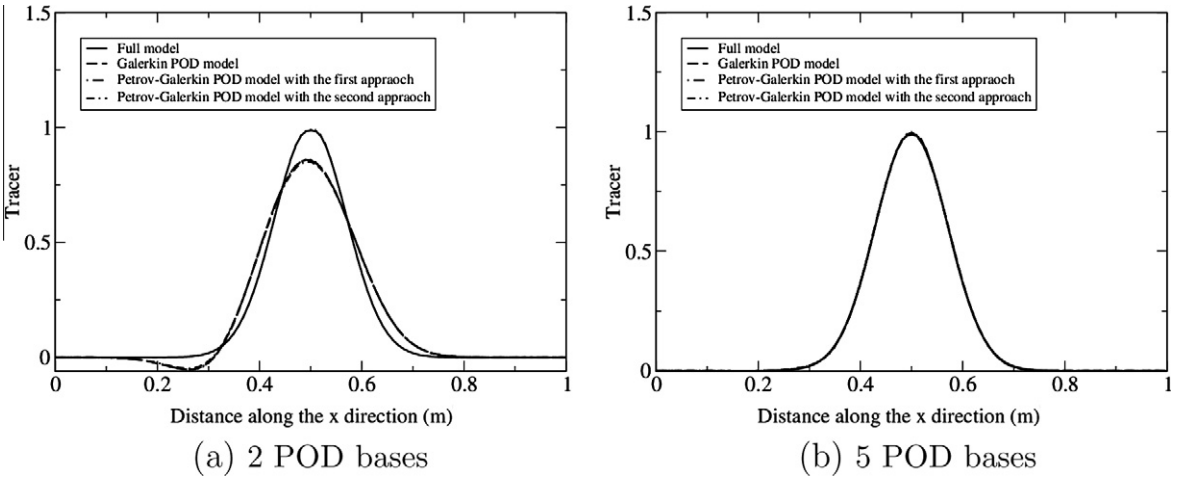

Fig. 9. Case 2 (1D Gaussian wave): comparison of results between the full and POD models (where the first approach (60); and the second approach (64) used with (72), 5 POD bases represent 98.4% of the original energy while 2 POD bases represent 80% of the original energy).

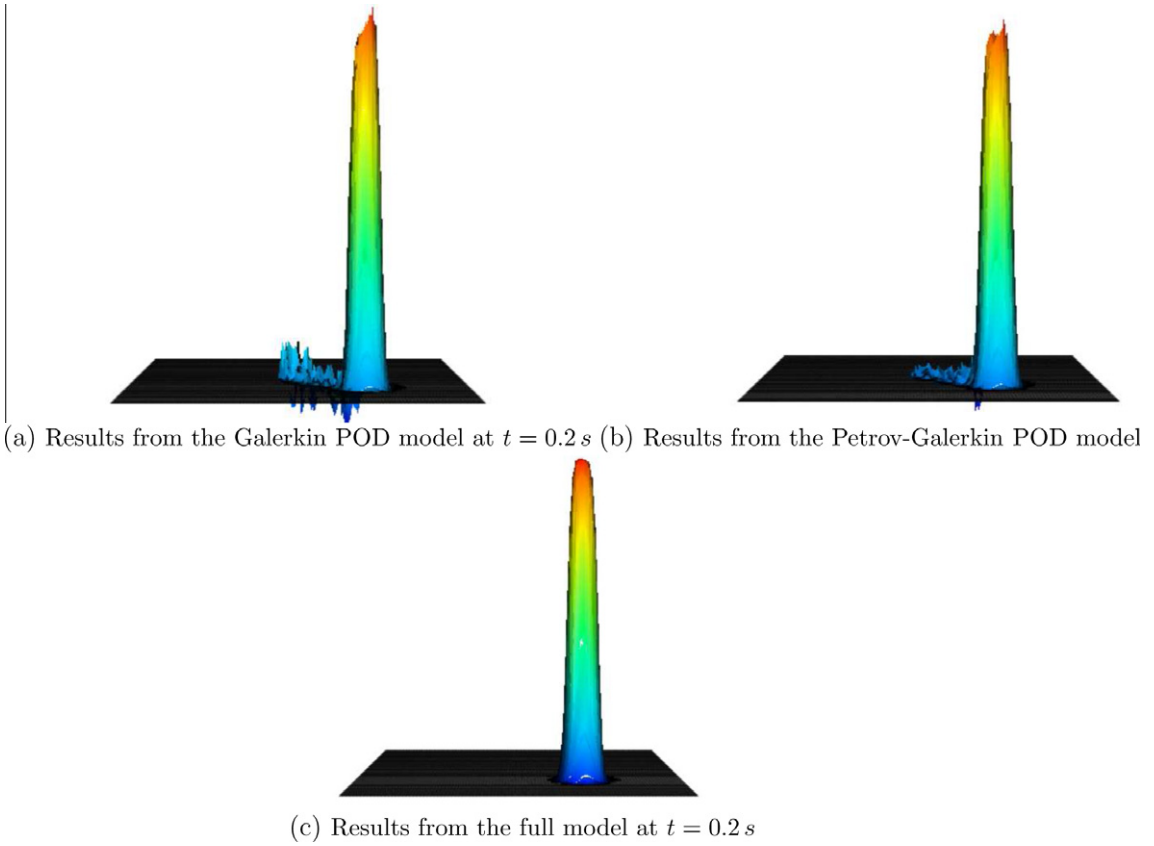

Fig. 10. Case 3 (2D 45° advection): comparison of the results obtained from the POD models and full model, where 15 POD bases are used, which represent 95% of the original energy.

A comparison between the POD and full model results is displayed in Figs. 10 and 11. It can be seen that the POD reduced order results using the Galerkin approach become oscillatory and unstable and the RMSE of results increases as the simulation time increases. By using the Petrov–Galerkin POD approach, the RMSE and relative error of results are reduced by a factor of 2 during the integration period [0.05 s,0.2 s] while the correlation coefficient increases from 99.8% to 99.95%.

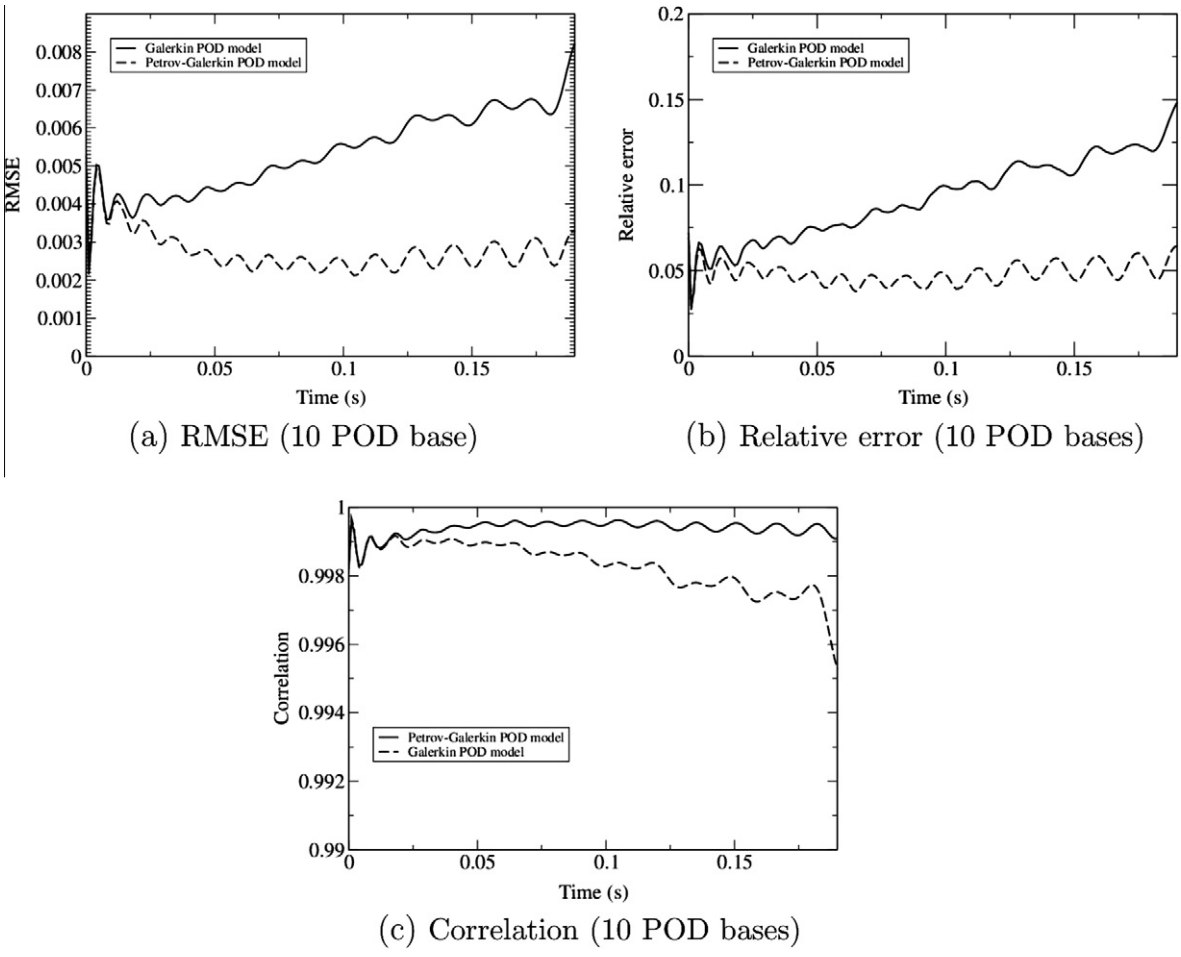

Fig. 11. Case 3 (2D 45° advection): RMSE and correlation coefficient of tracer results between the POD and the full models.

7. Conclusions

A new Petrov–Galerkin method for stablisation of high order nonlinearity in reduced order modelling is developed. The POD discontinuous Galerkin (DG) reduced order model is applied to 1D and 2D advection, and 1D shock wave cases. A comparison of the results between the POD models using the Petrov–Galerkin and traditional Galerkin approaches is carried out. It is observed that the instability in the POD results is reduced by using the Petrov–Galerkin POD methods which naturally introduces a diffusion term into ROM. The RMSE of results between the POD and full models is decreased by 15%–60% while the correlation coefficient is mostly larger than 98%–99.5% when the Petrov–Galerkin approach is used in conjunction with ROM. The Petrov–Galerkin POD model does well in capturing and resolving discontinuities of shock waves. The results obtained reproduce the correct density and velocity profiles of the rarefaction wave.

Future work will investigate impact of DEIM methodology on additional economy in CPU time (due to nonlinear effects) and apply this new Petrov–Galerkin POD approach to more complex fluid flow models and optimal control of shock waves for the Sod problem [18]. We envisage to compare in future research work the new approach with the calibration method, *e.g.* Noack's method [23–25] (which matches the cascade of energy in the reduced order model with that of the high fidelity model) and the method proposed by Wang et al. [26].

Acknowledgments

This work was carried out under funding from the UK's Natural Environment Research Council (Projects NER/A/S/2003/00595, NE/C52101X/1 and NE/C51829X/1), the Engineering and Physical Sciences Research Council (GR/R60898 and EP/I00405X/1), and with support from the Imperial College High Performance Computing Service. Prof. I.M. Navon acknowledges the support of NSF/CMG Grant ATM-0931198. Dr. Juan Du acknowledges the support of National Natural Science Foundation (Grant No. 41075064) and National Basic Research Program of China (Grant No. 2012CB417404), and support from

Prof. Zhu. We would like to thank three reviewers and editors for their contribution to improvement of the paper and in depth useful and constructive comments.

Appendix A. Derivation of POD DG diffusion coefficient

The Petrov–Galerkin modified form of the differential Eq. (32) is re-written here:

$$(I - (\nabla_{xt} \cdot A^*_{xt})^T P^*_{xt})(A_{xt} \cdot \nabla_{xt} \Psi - s) = 0. \tag{A.1}$$

Multiplying (A.1) by a space–time basis function N_{xti} and integrating by parts over a single element V_E (here DG methods are employed), a general form of the Petrov–Galerkin operator for finite element methods is:

$$\int_{V_E} N_{xti}(I - (\nabla_{xt} \cdot A^*_{xt})^T P^*_{xt}) r \, dV. \tag{A.2}$$

The finite element Riemann method is defined with [28]

$$P^*_{xt} = \frac{h}{2} |n_x A^*_x + n_y A^*_y + n_z A^*_z|^{-1}, \tag{A.3}$$

where h is the length size of the element. This is the approach used with Riemann solvers that are implemented with a control volume discretisation in which case (n_x, n_y, n_z) is the direction normal to a control volume. For finite elements $n_x = N_{ix}/n, n_y = N_{iy}/n$ and $n_z = N_{iz}/n$ where n_* is the normalisation factor. It should be noted that the transport term premultiplied by I when integrated by parts is conservative and has much in common with control volume methods. Using the basis functions to define the length scale $\frac{h}{2}$ associated with the basis functions one can eliminate out the normalisation factor to obtain:

$$P^*_{xt} = |N_{xtix} A^*_x + N_{xtiy} A^*_y + N_{iz} A^*_z|^{-1} = |A^*_{xt} \cdot \nabla_{xt} N_{xti}|^{-1}. \tag{A.4}$$

This is important as applying this method to reduced order basis functions there is no well defined length scale except through this gradient of the basis functions.

Since the POD matrices may be relatively small one can manipulate their eigen structure in order to construct stabilization methods. For example, for calculation of the matrix B (defined in Eq. (69)), we have

$$\int_{V_E} N^{POD}_{xti}((\nabla_{xt} \cdot A^*_{xt})^T P^*_{xt}) r \, dV \approx (B^{POD^T} O^{POD^{-1}} l^{POD})_i, \tag{A.5}$$

with

$$l^{POD}_i = \int_{V_E} N^{POD}_{xti} r dV, \tag{A.6}$$

$$O^{POD^{-1}} = \beta \frac{1}{4} |B^{POD}|^{-1} = \beta \frac{1}{4} R_{B^{POD}} |\Lambda_{B^{POD}}|^{-1} L_{B^{POD}}. \tag{A.7}$$

$R_{B^{POD}}, L_{B^{POD}}$ are matrices of right and left eigen-vectors of B^{POD} and $\Lambda_{B^{POD}}$ is the matrix of eigen-values of B^{POD}. A possible alternative to $O^{POD^{-1}}$ which would ensure positive diffusion is:

$$O^{POD^{-1}} = \beta \frac{1}{4} (B^{POD^T} B^{POD})^{-\frac{1}{2}}. \tag{A.8}$$

Now since $(B^{POD})_i$ is analogous to $N^{POD}_{xti} \cdot \nabla_{xt} A^*_{xt}$ of (A.5), $(l^{POD})_i$ is analogous to r of (A.5), and $O^{POD^{-1}}$ is analogous to P^*_{xt} they replace them in the definition of the diffusion coefficient in Eq. (42) which then results in Eq. (64).

References

[1] F. Fang, C.C. Pain, I.M. Navon, M.D. Piggott, G.J. Gorman, P. Allison, A.J.H. Goddard, Reduced order modelling of an adaptive mesh ocean model, Int. J. Numer. Methods Fluids 59 (8) (2009) 827–851.
[2] I. Hoteit, A. Kohl, Efficiency of reduced-order, time-dependent adjoint data assimilation approaches, J. Oceanogr. 62 (4) (2006) 539–550.
[3] P.T.M. Vermeulen, A.W. Heemink, Model-reduced variational data assimilation, Mon. Wea. Rev. 134 (2006) 2888–2899.
[4] C. Robert, E. Blayo, J. Verron, J. Blum, F.X. Le Dimet, Reduced-order 4d-var: a preconditioner for the incremental 4d-var data assimilation method, Geophys. Res. Lett. 33 (2006). pp. L18609-1–4.
[5] A.C. Antoulas, Approximation of Large-scale Dynamical Systems, Book Series: Advances in Design and Control, DC 06, SIAM, Philadelphia, 2005.
[6] M. Rewienski, J. White, A trajectory piecewise-linear approach to model order reduction and fast simulation of nonlinear circuits and micromachined devices, IEEE Trans. Comput. Aided Des. Integr. Circuits Syst. 22 (2) (2003) 155–170.
[7] K. Willcox, J. Peraire, Balanced model reduction via the proper orthogonal decomposition, AIAA J. 40 (11) (2002) 2323–2330.
[8] F. Bassi, S. Rebay, A high-order accurate discontinuous finite element method for the numerical solution of the compressible Navier–Stokes equations, J. Comput. Phys. 131 (1997) 267–279.
[9] M. Bergmann, C.H. Bruneau, A. Iollo, Enablers for robust POD models, J. Comput. Phys. 228 (2) (2009) 516–538.
[10] F. Fang, C.C. Pain, I.M. Navon, M.D. Piggott, G.J. Gorman, P. Allison, A.J.H. Goddard, A POD reduced order unstructured mesh ocean modelling method for moderate Reynolds number flows, Ocean Model. 28 (1–3) (2009) 127–136.

Please cite this article in press as: F. Fang et al., Non-linear Petrov–Galerkin methods for reduced order hyperbolic equations and discontinuous finite element methods, J. Comput. Phys. (2012), http://dx.doi.org/10.1016/j.jcp.2012.10.011

[11] A. Iollo, S. Lanteri, J.A. Desideri, Stability properties of POD-Galerkin approximations for the compressible Navier–Stokes equations, Theor. Comput. Fluid Dyn. 13 (2000) 377–396.
[12] B. Galletti, C.H. Bruneau, L. Zannetti, A. Iollo, Low-order modelling of laminar flow regimes past a confined square cylinder, J. Fluid Mech. 503 (2004) 161–170.
[13] B. Kragel, Streamline Diffusion POD Models in Optimization, Dissertation, Fachbereich IV Universit ät Trier, 2005.
[14] B.R. Noack, M. Schlegel, B. Ahlborn, G. Mutschke, M. Morzyński, P. Comte, G. Tadmor, A finite-time thermodynamics of unsteady flows, J. Non-equilib. Thermodyn. 33 (2) (2009) 103–148.
[15] N.C. Nguyen, J. Peraire, An efficient reduced-order modeling approach for non-linear parametrized partial differential equations, Int. J. Numer. Methods Eng. 76 (2008) 27–55.
[16] K. Carlberg, C. Bou-Mosleh, C. Farhat, Efficient non-linear model reduction via a least-squares Petrov–Galerkin projection and compressive tensor approximations, Int. J. Numer. Methods Eng. 86 (2011) 155–181.
[17] P. Bochev, M. Gunzburger, Least Squares Finite Element Methods, Springer, Berlin, 2009.
[18] Chris Homescu, I.M. Navon, Optimal control of flow with discontinuities, J. Comput. Phys. 187 (2003) 660–682.
[19] A.G. Buchan, S.R. Merton, C.C. Pain, R.P. Smedley-Stevenson, Riemann boundary conditions for the Boltzmann transport equation using arbitrary angular approximations, Ann. Nucl. Energy 38 (2011) 1186–1195.
[20] J. Donea, A. Huerta, Finite Element Methods for Flow Problems, John Wiley & Sons Ltd., Chichester, UK, 2003.
[21] G.A. Sod, Survey of several finite difference methods for systems of nonlinear hyperbolic conservation laws, J. Comput. Phys. 27 (1978) 1–31.
[22] A. Iollo, Remarks on the Approximation of the Euler Equations by a Low Order Model, INRIA, Report of research, RR-3329, 1997.
[23] B.R. Noack, R. Papas, P. Monkewitz, The need for a pressure-term representation in empirical Galerkin models of incompressible shear flows, J. Fluid Mech. 523 (2005) 339–366.
[24] B.R. Noack, K. Afanasiev, M. Morzyński, G. Tadmor, F. Thiele, A hierarchy of low-dimensional models of the transient and post-transient cylinder wake, J. Fluid Mech. 497 (2003) 335–363.
[25] B.R. Noack, M. Schlegel, M. Morzyński, G. Tadmor, System reduction strategy for Galerkin models of fluid flows, Int. J. Numer. Methods Fluids 63 (2) (2010) 231–248.
[26] Z. Wang, I. Akhtar, J. Borggaard, T. Iliescu, Proper orthogonal decomposition closure models for turbulent flows: a numerical comparison, Comput. Methods Appl. Mech. Eng. 237–240 (2012) 10–26.
[27] E.F. Toro, Riemann Solvers and Numerical Methods for Fluid Dynamics, A Practical Introduction, third ed., Springer, Berlin, 2009.
[28] C.C. Pain, M.D. Eaton, R.P. Smedley-Stevenson, A.J.H. Goddard, M.D. Piggott, C.R.E. de Oliveira, Streamline upwind Petrov–Galerkin methods for the steady-state Boltzmann transport equation, Comput. Methods Appl. Mech. Eng. 195 (2006) 4448–4472.

Please cite this article in press as: F. Fang et al., Non-linear Petrov–Galerkin methods for reduced order hyperbolic equations and discontinuous finite element methods, J. Comput. Phys. (2012), http://dx.doi.org/10.1016/j.jcp.2012.10.011